OPPORTUNISTIC LARGE ARRAY (OLA)-BASED ROUTING FOR SENSOR AND ADHOC WIRELESS NETWORKS

A Dissertation
Presented to
The Academic Faculty

By

Lakshmi V Thanayankizil

In Partial Fulfillment
Of the Requirements for the Degree
Doctor of Philosophy in the School of Electrical and Computer Engineering

Georgia Institute of Technology
December 2013

OPPORTUNISTIC LARGE ARRAY (OLA)-BASED ROUTING FOR SENSOR AND ADHOC WIRELESS NETWORKS

Approved by:

Dr. Mary Ann Weitnauer, Advisor
School of Electrical and Computer Engineering
Georgia Institute of Technology

Dr. Raghupathy Sivakumar
School of Electrical and Computer Engineering
Georgia Institute of Technology

Dr. Douglas Blough
School of Electrical and Computer Engineering
Georgia Institute of Technology

Dr. Edward Coyle
School of Electrical and Computer Engineering
Georgia Institute of Technology

Dr. Tom Morley
School of Mathematics
Georgia Institute of Technology

Date Approved: October. 9, 2013

To Vallikkat Thanayankizil Sarojini Amma, my dearest Mutassi

ACKNOWLEDGEMENTS

It is a pleasure to thank the many people who made this thesis possible. First and foremost, I would like to thank my advisor, Dr. Mary Ann Weitnauer, for her patience, genuine care and concern, and faith in me. With her enthusiasm, her inspiration, and her great efforts to explain complex concepts clearly and simply, she has helped to make PhD fun for me. It has been an honor to work under her, and be her first female PhD student. Her patience, flexibility, genuine caring and concern, and faith in me during the dissertation process enabled me to attend to life while also earning my PhD. She has been motivating, encouraging, and enlightening. She has never judged nor pushed when she knew I needed to juggle priorities. I am also thankful for the excellent example she has provided as a successful woman engineer and professor. Her flexibility in scheduling, gentle encouragement and relaxed demeanor made for a good working relationship and the impetus for me to finish. I would be indebted to her my whole life, and if I have imbibed any of her personality during these years, I feel blessed.

I also thank the members of my thesis committee, Prof. Raghupathy Sivakumar, Professor Douglas Blough and Dr. Ed Coyle for being on my thesis reading committee. Their encouragement and enlightening suggestions have greatly improved my research and this dissertation. I express my appreciation to Prof. Morley for being on my dissertation committee. A big part of my PhD learning experience has been the interaction and collaboration with fellow students at Georgia Tech. I have had wonderful lab-mates at Smart Antenna Research Lab. In particular my discussions with Aravind Kailas, Alper Akanser, and Jinwoo Jung, have benefitted me a lot. I would also like to thank them for

making the work environment at SARL very enjoyable. I would like to thank the current members of SARL, Haejoon Jung, Jian Lin, Van Ngyuyen, Yong Jun Chang for their valuable comments to my dissertation. Ms. Cordai Farrar and Ms. Jackqeline Trappier were of immense help in getting all the forms and documents in, especially since I was out of state. I would like to thanks my colleagues at General Motors, Dr. Fan Bai and Dr. Timothy Talty for always motivating me to focus and work hard on my thesis while I was working at General Motors R&D. Their encouragement certainly helped me finish my thesis sooner. I thank them for being very understanding and allowing me to take time off from work to work on my thesis.

Finally, I would like to thanks my husband Sandeep Menon, for encouraging and supporting me throughput my PhD, and my son Siddharth Menon for being the joy in my life and the most precious gift from God. I would like to thank my parents who are miles away, but whose prayers give me the strength to move on. I would like to thank them for teaching me not to give up, and face all hassles with a smile.

Thank you for everything. To you, I dedicate this work.

TABLE OF CONTENTS

LIST OF TABLES

LIST OF FIGURES

SUMMARY

An Opportunistic Large Array (OLA) is a form of cooperative diversity in which a large group of simple, inexpensive relays operate without any mutual coordination, but naturally fire together in response to the energy received from a single source or another OLA. The main contributions of this thesis are the introduction of two OLA-based routing protocols: OLA Concentric Routing Algorithm (OLACRA), which is an upstream routing algorithm suitable for static wireless sensor networks (WSNs), and OLA Routing On-Demand (OLAROAD), which is a robust reactive routing scheme suitable for mobile ad hoc networks (MANETs). In fixed multi-hop wireless sensor networks with a single sink, where energy conservation is often a concern, simulations of the new algorithms show as much as 80% of the transmit energy required to broadcast data can be saved, relative to existing OLA-based broadcasting approaches. In MANETs, where robustness of the routes is an important performance indicator, OLAROAD-based cooperative routes last much longer compared to their state-of-art multi-hop non-cooperative transmission (CT)-based counterparts. However, OLACRA and OLAROAD have higher node participation, and thereby lower throughput, in comparison with the non-CT schemes. To improve the throughput, and thereby bandwidth utilization, the properties of uplink OLAs and their suppression regions are carefully studied. Based on the observations, Hop-Optimized OLACRA (HOLA), which is a variant of OLACRA, and has the maximum bandwidth utilization amongst all the OLA unicast schemes studied, is proposed. HOLA routes have bandwidth utilization comparable to non-CT schemes, but a much lower (~10 dB less) transmit power per node.

The last section of this thesis treats the MAC design for OLA-based networks. In contrast to non-CT networks, a 802.11-based RTS/CTS MAC scheme is shown to reduce the reliability in OLA unicast schemes. A distributed cluster-head-based MAC scheme for channel reservation and OLA Size Adaptation Mechanism for link repair/maintenance are proposed for OLA-based networks. The performances of these protocols are shown to be comparable to a non-CT multihop scheme using the RTS/CTS/DATA/ACK handshake-based link layer design.

CHAPTER 1

INTRODUCTION

Some wireless sensor networks (WSN), like intra-vehicular WSNs, battle field WSNs etc consist of a large number of wireless sensor nodes that are usually densely and randomly deployed for unattended operation. For these networks, the sensors are battery-powered, and hence an important design issue is the amount of the energy available at each node, requiring WSNs to have energy-efficient routing schemes and transmission algorithms. This thesis presents an energy-efficient routing approach that is based on a physical layer that uses cooperative transmission (CT).

CT is the strategy wherein one user helps another user transmit multiple copies or versions of the same message through independently faded channels, to ultimately be received by a destination node [1, 2]. By sharing information this way, the users can create a "virtual array" [3] and achieve spatial array and diversity gain. Because of the diversity gain, all users can reduce their fade margins (i.e., their transmit power) by as much as 12-15 dB, thereby reducing the energy consumed by each transmitter [3]. Because of the array gain (the simple summing of average powers from each antenna), the required transmission power for a link can be divided across multiple radios; this provides a convenient mechanism for applications in which each node has extreme transmit power constraints or heat restrictions.

A particularly simple form of CT called the Opportunistic Large Array (OLA) [4] avoids individual node addressing and is therefore scalable with node density and suitable

for highly mobile networks. An OLA is formed when nodes transmit the same message, without coordination between each other, but at approximately the same time in response to the energy received from a single source or another OLA [5, 6]. The signal received from an OLA has the same model as a multi-path channel [5]. Small time offsets (because of different distances and processing delays) and small frequency offsets (because each node has a different oscillator frequency) are like excess delays and Doppler shifts, respectively. As long as the receiver, such as a rake receiver, can tolerate the effective delay and Doppler spreads of the received signal, decoding can proceed normally. OLAs and OLA-based networking have been demonstrated in testbeds in [40].

To induce the orthogonalization necessary to create diversity channels, nodes transmitting to rake receivers can intentionally delay their transmissions (to emulate a frequency selective channel) [7] or nodes with orthogonal frequency division multiplexing (OFDM) transmitters can choose different sub-carriers. Alternatively, space-time block coding (STBC) can be implemented [8], where nodes can randomly choose which part of the STBC code they will transmit. Even though many nodes may participate in an OLA transmission, energy is saved relative to single-node transmissions because all nodes can reduce their transmit powers dramatically and large fade margins are not needed. Further in [6], the simple OLA broadcast method, which is called Basic OLA, was shown to yield a transmit energy savings of over 5dB compared with the Broadcast Incremental Power (BIP) algorithm [9].

The first contribution of this thesis is OLA Concentric Routing Algorithm (OLACRA), which is an upstream routing method that is appropriate for WSNs that use OLA-based CT, and are characterized by a sink or fusion node in the center of a large,

dense deployment of energy-constrained nodes [10]. OLACRA exploits the concentric structure of OLAs that are naturally created in the previous broadcast to limit the size of the upstream OLAs and guide them back to the sink. OLACRA requires neither location knowledge nor centralized control for the pre-computing of routes. Further energy can be saved through the use of a transmission threshold [11]. This variant of OLACRA is called OLACRA with Transmission Threshold (OLACRA-T) [12]. Finally, an important feature that all the proposed schemes inherit from Basic OLA is that no individual nodes are addressed. This makes the protocols scalable with node density.

Variants of OLACRA-T that enhance the upstream connectivity called OLACRA with Flooding and Threshold (OLACRA-FT) and OLACRA-FT with variable relay power (OLACRA-VFT) are also presented [13]. The downlink transmission is optimized to obtain fixed step-sizes in OLACRA with Step-size Control (OLACRA-SC) and energy savings of over 90 percent relative to Basic OLA is reported in this scheme. These are analyzed for deterministic channels [11] where node transmissions are on orthogonal non-faded channels, and for diversity channels where transmissions are on faded limited orthogonal channels. Intentional delay dithering with rake receivers is done at the transmitter nodes to provide diversity gain at the receiver in diversity channels [14]. The algorithms presented are analyzed using Monte Carlo simulations.

OLAROAD is an OLA-based reactive routing protocol proposed for Mobile Ad Hoc Networks (MANETs). A MANET is a self-configuring network of mobile wireless nodes, in an arbitrary topology with no existing infrastructure. Because of node mobility, the topology changes rapidly and hence MANETs require reactive routing protocols, which compute routes on the fly. Traditional CT-based reactive routing schemes preselect the

cooperators as part of the routing, which results in high levels of overhead and is not scalable. In contrast, the proposed OLAROAD scheme avoids these scalability problems, because no nodes are individually addressed (aside from the source and destination nodes), and the complexity of the proposed scheme is independent of node density, given the density is high enough to support OLA transmission [4]. Also, there is no centralized control and no coordination between pairs of individual relay nodes. In other words, the proposed scheme requires no explicit medium access control (MAC) function for a single flow; copies of the packet from multiple simultaneously transmitting nodes are exploited to attain an SNR advantage through diversity combining [4]. That an OLA, or "virtual array," occupies an area rather than a single point is one reason why OLA-based routing is tolerant of limited node motion. Another distinction is that in OLAROAD, CT is incorporated in both the route set-up and data transmission phases, whereas in all existing CT schemes, cooperation is done only in the data transmission phase. The performance of OLAROAD is compared to a traditional reactive protocol called Ad Hoc On Demand Distance Vector (AODV), and the benefits of OLAROAD in mobile and highly dense areas is shown.

Many aspects of OLA transmission and OLA routing have been explored recently in [38,39,40,41]. However, these works do not compare the spatial reuse of networks that use OLA routing with networks that use non-CT routing schemes. OLA routes/ flows typically have higher node participations and hence larger suppression regions (and lower bandwidth utilizations) than non-CT flows. The inter-flow, intra-flow and intra-OLA suppressions, are different from other non-CT and CT routing schemes. The intra-flow contention of OLA unicast flows and the optimum packet insertion rate have been analyzed

for a strip network using the continuum assumption in [40]; however the strip network assumption abstracts the asymmetry and hop dependency of OLAs. We show that the suppression regions of OLAs are asymmetric and hop-dependent for random networks and the step-width grows with the uplink level index for OLACRA-SC. To remedy these problems, Hop-Optimized OLA (HOLA), a variant of OLACRA-SC, is presented in this thesis. HOLA reduces hop asymmetries and has the highest bandwidth utilization amongst all OLA upstream schemes.

The last section of this thesis presents a Data Link Layer scheme for OLA networks with multiple flows. Since no intermediate nodes are individually addressed in OLA routes, the design of link level MAC schemes is more challenging. In contrast to multihop non-CT networks, a handshake-based Carrier Sense Multiple Access (CSMA) will reduce the reliability in OLA networks. A new cluster-head-based MAC scheme for channel reservation and OLA Size Adaptation Mechanism for link maintenance are proposed for OLA-based networks. To the best knowledge of the authors, this is the first MAC layer scheme proposed for OLA-based cooperative networks. The performances of these protocols are studied in comparison with CSMA-based MAC layer schemes used in non-CT multihop networks. The CH-based OLA routes are shown to have reliability comparable to CSMA-based multihop networks. Additionally, the OLA Size Adaptation Mechanism is shown to achieve communication reliability (by performing link repair) in segmented energy-constrained networks, where the link repair schemes of existing CT and non-CT networks fail. Careful observations on the benefits of OLA routing, and the kinds of networks where OLA routing has maximum benefits are also reviewed.

Summarizing, this thesis makes the following contributions:

- Presents OLACRA, which is an upstream routing protocol suitable for wireless sensor networks. OLACRA is the first OLA-based upstream scheme proposed for WSNs, and saves over 90 percent of the energy compared to Basic OLA schemes without requiring any centralized control.
- Presents OLAROAD, which is an OLA-based reactive routing protocol suitable for MANETs. OLAROAD routes, on comparison with traditional non-CT multihop routing schemes (like AODV), is invariant to changes in density. OLAROAD routes require fewer route refreshes/ local repairs and have lower end-to-end delay (for single packet/single flow networks), making them suitable for mobile networks with low network traffic.
- Presents HOLA, which is a contention-aware OLA routing scheme, suitable for networks with multiple flows and multiple packets per flow. The Bandwidth utilization of HOLA is comparable to non-CT multihop schemes, and much higher compared to Basic OLA and OLACRA/ OLAROAD. For similar end-to end delay and bandwidth utilization, the transmit power of individual nodes in HOLA is much lower than non-CT schemes.
- Presents a cluster-head-based ACK scheme for link/route reliability in OLA routes. CSMA-based schemes, which are traditionally used for wireless networks, are shown to work very poorly for OLA unicast routes (PDR of 0.5). The reliability of CH-ACK is much higher at 0.9, and is comparable to the reliability that CSMA-based MAC provides in non-CT multihop networks. The increased reliability is achieved at a higher overhead required in establishing the CH ACK mechanism.

- Presents OLA Size Adaptation Mechanism, which is a link repair mechanism proposed for OLA networks. The proposed scheme has two benefits over existing link repair mechanisms proposed for CT and non-CT multihop schemes: (1) OLA Size Adaptation triggers link repair only after ensuring the link has broken (i.e. majority of the nodes in the OLA did not receive an ACK), unlike some CT-based ACK schemes which trigger link repair if the CH doesn't receive ACK, (2) OLA Size Adaptation can maintain reliability and overcome large network holes/partitions, where traditional link/routing schemes fail. Data Link Layer design based on OLA Size Adaptation Mechanism and CH-based MAC is the first data link layer design proposed for OLA networks.

CHAPTER 2

LITERATURE REVIEW

A large number of battery powered WSNs are inherently multi-hop because the range of the highly energy-constrained low power nodes is small compared to the areas requiring coverage. A common approach at the network layer to the energy-efficiency problem is energy-aware routing. The objective of energy-aware protocols has been either minimizing the energy consumption or maximizing the network lifetime. The aim of minimum-energy routing [15, 16, 17] is to minimize the total consumed energy to reach the destination, which in turn minimizes the energy consumed per unit flow. This method does not yield long network life because if all the traffic is routed through the same minimum-energy path, the batteries of the nodes along the path will drain quickly, while the other nodes will remain intact. On the other hand, the objective of the maximum network lifetime scheme [18, 19, 20, 21] has been to increase the time to network partition. It turns out that to maximize the network lifetime, the traffic should be routed such that the energy consumption is balanced among the nodes in proportion to their energy reserves [18]. However the above-mentioned energy-aware protocols do not consider cooperation among nodes.

Lately CT has been extended to multi-hop networks to further enhance the energy savings. Several works in this area assume that a conventional multi-hop route has already been identified and power is allocated to the nodes along or near the route to assist with cooperative transmission [22, 23, 24]; the corresponding routing metric is the total path power. A particularly well-developed example is proposed by Jakllari et al [25]. They

proposed a protocol that selects relays from among the nodes in a conventional route (the "primary path"), and uses cooperative transmission to take longer hops along that same route. As another example, [24] considers a sequence of node clusters between the source and destination (presumably along a pre-determined route). They select one relay from each cluster to minimize the probability of outage, either hop-by-hop, or end-to-end. One disadvantage of using these schemes is that they require coordination and addressing of relay nodes, which OLA-based schemes do not entail.

In OLA-based networks, routing is generally established using flooding [26], which is not energy-efficient for upstream routing. The only work other than OLACRA, which limits flooding in the upstream was done in [27], where the nodes are assumed to be aware of their location, which is obtained using a global positioning system (GPS). However this assumption might not be practical in WSNs. OLACRA on other hand does not require location information.

In fading channels, an OLA can provide spatial diversity if the waveforms transmitted by the different nodes in the OLA are orthogonal and the receivers can receive on those orthogonal dimensions and do diversity combining. The authors in [5] considered the case when all the waveforms were orthogonal to each other and the receivers could separate all transmissions and do optimal diversity combining.

Delay-dithering schemes to orthogonalize transmissions were proposed in [7, 28]. Wei et al. considered a limited-orthogonal scheme in [28], where every relay node delays its transmission by a random "artificial delay" selected from a pool of artificial delays {0, T, 2T, …, (*m-1*)T}. This scheme converts the channel into *m* orthogonal channels which can be combined at the receiver. $m < n$ where n is the total number of transmitting nodes.

Another work was done in [8], where space-time codes were used to orthogonalize channels of the nodes in OLA-based networks.

The authors in [5] also considered a case when all nodes transmitted on the same channel (non-orthogonal). Although most authors make node transmissions orthogonal to improve performance, authors in [5] showed that non-orthogonal transmissions outperformed the orthogonal case. This is because in a dense node deployment, although the probability of having a good fading realization is very small, there is always a fraction of nodes that experience them and they boost the overall performance of the system.

Most of the existing CT-based ad hoc routing protocols assume that a conventional multi-hop route already exists or that clusters have somehow already been defined [22, 23, 24, 25]. However, approaches that require a pre-existing route lead to additional overhead in MANETs. More recently, opportunistic CT-based routing schemes have also been proposed [32, 33, 34], where the actual forwarding cooperators are not pre-determined, but decided on the fly, based on signal strength measurements, NACK signals and assigned priorities. However [32] assumes an existing multi-hop route, and [33, 34] must identify a list of potential cooperators before the actual transmission begins. None of these schemes, unlike OLAROAD, will avoid the high levels of complexity, overhead, and delay required to do multi-hop routing in mobile networks.

Concurrent cooperative transmissions (CCT) (similar to OLA) have gained popularity recently, and have been considered in [38,39,40,41]. However, these works don't compare the spatial reuse of OLAs with non-CT flows. OLAs typically have higher node participations and hence larger suppression regions (and lower bandwidth utilizations) than non-CT networks. These result in inter-flow, intra-flow and intra-OLA

suppressions, which significantly degrade the bandwidth utilization. The intra-flow contention of OLA unicast flows, and the optimum packet insertion rate has been analyzed for a strip network using the continuum assumption in [40]; however the strip network assumption abstracts the asymmetry and hop dependency of OLAs. The suppression regions of OLAs are asymmetric and hop-dependent for random networks and the step-width grows with the uplink level index for OLACRA-SC. Hop-Optimized OLA (HOLA), a variant of OLACRA reduces hop asymmetries and has the highest bandwidth utilization amongst all OLA upstream schemes.

CHAPTER 3

OLACRA

3.1 SYSTEM MODEL

The nodes are assumed to be half-duplex and distributed uniformly and randomly over a continuous area with average density ρ. It is assumed that a node can decode and forward (D&F) a message without error if the node's received signal-to-noise ratio (SNR) is greater than or equal to a modulation-dependant threshold [4]. Assumption of unit noise variance transforms the SNR threshold to a received power criterion, which is denoted by the decoding threshold, τ_d. The decoding threshold τ_d is not explicitly used in real receiver operations. A real receiver always just tries to decode the message. If no errors are detected, then it is assumed that the receiver power must have exceeded τ_d. In contrast, the proposed transmission threshold would be explicitly compared to an estimate of the received SNR.

Let the normalized source power, relay transmit power, and the relay transmit power per unit area be denoted as P_s, P_r and $\overline{P}_r = P_r\rho$ respectively. The path-loss function in Cartesian coordinates is given by $l(x, y) = \left(x^2 + y^2\right)^{-1}$, where (x, y) are the normalized coordinates at the receiver. As in [5], distance d is normalized by a reference distance d_o. Let power P_o be the received power at d_o. The received power from a node distance d away is $P_{rec} = \min(\frac{P_o}{d^2}, P_o)$.

Two network models are considered, the deterministic model and the diversity channel model. In the deterministic model, the power received at a node is the sum of the powers

received from each of the node transmissions. This model implies that the node transmissions occur on orthogonal non-faded channels. In the diversity channel model, node transmissions are assumed to be on limited number of orthogonal Rayleigh-faded channels.

In the deterministic channel model, it is assumed that if a set of relay nodes (say L_n) transmits simultaneously, the node j with normalized coordinates (x_o, y_o) receives with power

$$P_{rec}^{J} = P \sum_{(x,y)\in L_n} l(x - x_o, y - y_o) \quad , \qquad (1)$$

where P is the normalized transmit power given by

$P = \frac{P_t G_T G_R}{\sigma_n^2} \left(\frac{\lambda}{4\pi d_0} \right)^2$, where P_t is the relay transmission power in mW, G_t and G_r are the transmit and receive antenna gains, σ_n^2 is the thermal noise power and λ is the wavelength in meters. Following [5], for ease of analysis a continuum of nodes is assumed, which means that the node density ρ is increased $(\rho \to \infty)$ while maintaining a constant $\overline{P}_r$. Then (1) simplifies to

$$P_{rec}^{J} = P \int_x \int_y l(x - x_0, y - y_o) dx dy \, . \qquad (2)$$

For the diversity channel model [14], the received power is given by

$$P_{rec}^{J} = \sum_{k=1}^{m} \gamma_k P_{rec,k}^{J} \quad , \qquad (3)$$

where m is the number of limited-orthogonal channels, and $P_{rec,k}^{J}$ is the average power received at the k^{th} orthogonal channel, and γ_k is a zero mean, unit variance exponential random variable.

The efficiency of Basic OLA was shown in [6] to depend on the decoding ratio (DR) defined in [13] as $\frac{\tau_d}{\overline{P}_r}$. In an earlier work, a device called the transmission threshold, τ_b, was found useful in limiting the node participation. A node tests its received SNR against τ_b, and if it exceeds τ_b, then the node does not participate. This test limits the participation to the "significant" boundary nodes, which are those nodes that can just barely decode. The quantity $10\log_{10}\frac{\tau_b}{\tau_d}$, referred to as the relative transmission threshold (RTT), defines the "window" in dB to allow for relaying. The algorithm OLA with Transmission Threshold or OLA-T is simply the application of RTT to OLA broadcasting [13]. With optimal τ_b, OLA-T was shown to save 32% of the transmit energy of a Basic OLA broadcast [13]. τ_b will be used in this thesis to make OLACRA more energy-efficient.

3.2 OLACRA

The OLA Concentric Routing Algorithm (OLACRA) has two phases. In the first phase, the sink initializes the network by flooding the whole network using OLA-T or OLA [5, 10]. In OLA-T the sink transmits waveform W_1 with power P_{sink}. "Downstream Level 1" or DL^1 nodes are those that can D&F the sink-transmitted message. Only the nodes in DL^1 whose received power is less than τ_b form the downlink OLA O_{D1}. The O_{D1}

nodes transmit a waveform, denoted by W_2 that carries the original message, but the waveform can be distinguished from the source transmission, for example, by using a different preamble, spreading code or center frequency. This difference enables nodes that can decode the W_2 waveform and which have not relayed this message before, to know that they are members of a new decoding level, DL^2.

A DL^2 node with received SNR less than τ_b forms O_{D2}, and relays using a different waveform W_3. This continues until each node is indexed with a particular level. A feature of Basic OLA and OLA-T algorithm is that the distance between inner and outer boundaries of a downstream OLA, also called the "step-size" [5], grows with the downstream OLA index. In other words, the rings that are farther from the sink are thicker.

The second phase of OLACRA is upstream communication. For upstream communication, a source node in DL^{n-1} transmits using W_n. Any node that can D&F at W_n will repeat at W_{n-1} if it is identified with DL^{n-1}, and if it has not repeated the message before. Downstream OLA boundaries formed in the initialization phase are shown by the dotted circles in Figure 1(a). Upstream OLAs formed are illustrated by the solid boundaries in Figure 1(b). Since only one level is ganged in the upstream, OLACRA as defined above, is also referred to as single-level OLACRA to differentiate it from the other ganging variations discussed later.

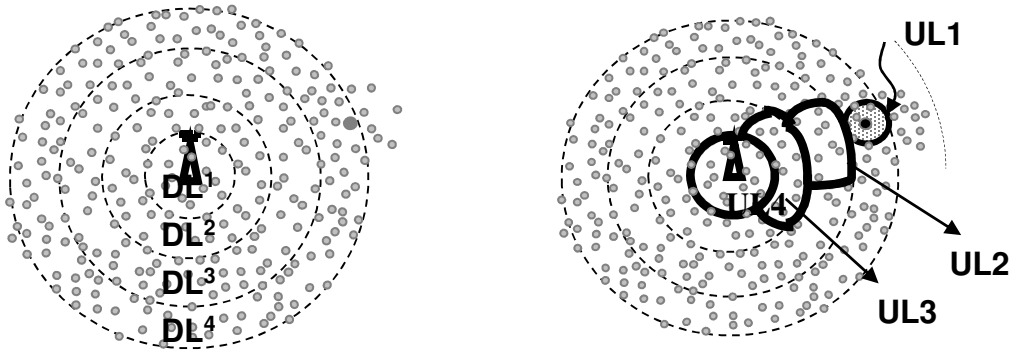

Figure 1: Illustration of OLACRA. (a) Phase 1 using OLA (b) and the upstream phase.

The n^{th} upstream OLA is referred to as UL^n, where UL^1 contains the source node. In Figure 1(b) for example, UL^1 is indicated by the solid circle and UL^4 contains the sink in the middle of the network. For OLACRA, the forward boundary of UL^n divides the nodes of UL^n from those that are eligible to be in UL^{n+1}. For a given message, to ensure that OLA propagation goes upstream or downstream as desired, but not both, a preamble bit is required. As in OLA-T, energy can be saved in OLACRA if the transmission threshold criterion is applied (i.e., only the nodes near the upstream forward boundary are allowed to transmit). In this case, O_{Uk} and UL^K would denote the transmitting set and decoding sets respectively for the k^{th} upstream level. This variant is called OLACRA-T. O_{Uk} and UL^K are the same in OLACRA (without a transmission threshold) as shown in Figure 1(b). Simulation example in Figure 2 illustrates OLACRA when the upstream source node is in DL^5. This plot is only for illustration purpose; the performance and benefits of OLACRA will be evaluated in Chapter 5.

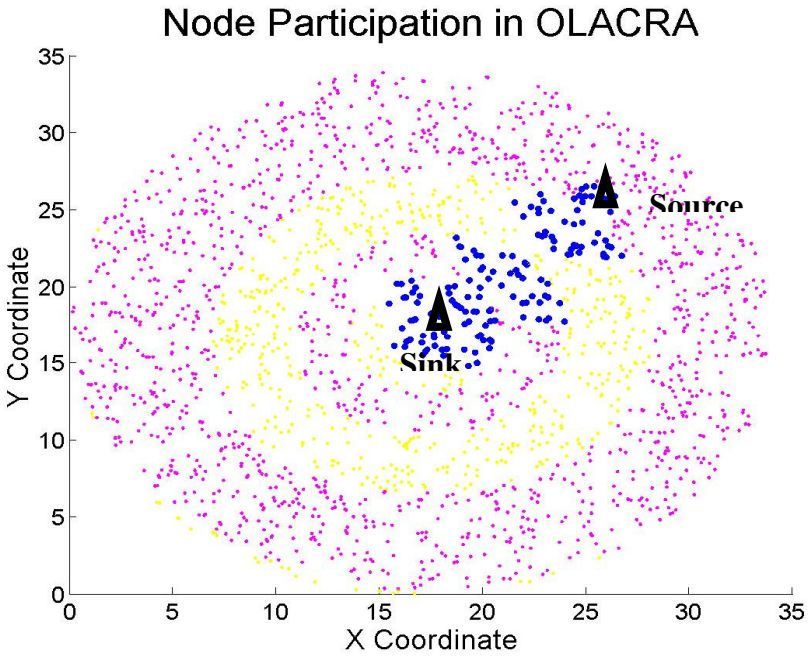

Figure 2: Node participation in single-level (Upstream nodes are denoted by the blue circles).

The two important performance issues in WSNs are energy-efficiency and reliability. Two metrics are defined to measure this in the context of OLACRA:

- Fraction of energy saved (FES) compares the transmit energy consumed by OLACRA with that of Basic OLA. FES is defined as

$$\text{FES} = 1 - \frac{\text{Total transmit energy consumed in the network in OLACRA}}{\text{Total transmit energy consumed in the network in Basic OLA}}.$$

- Packet delivery ratio (PDR) is the probability that a packet transmitted by the upstream source node is successfully decoded at the sink.

CHAPTER 4

ENHANCING OLACRA EFFICIENCY

4.1 UPSTREAM CONNECTIVITY ISSUES IN OLACRA

If the upstream source node is located far away from the sink, and also far away from the forward boundary of UL^1, then the decoding range of the source node maybe too short and UL^2 may not form. This can happen for an OLACRA upstream transmission when the source node is many, e.g. 7, steps away from the sink, because downlink levels of higher index are thicker. This causes the PDR to fall. This can be seen in Figure 3, which shows the node participation in OLACRA when the upstream source node is far away from the sink. The upstream source node is present near the forward boundary of DL^4 and the upstream transmission does not get to the sink in this case. This motivates the need to explore new methods to improve the upstream connectivity/reliability of OLACRA when the upstream source node is far away from the sink and also far away from the downstream reverse boundary. Methods that enhance the upstream connectivity and conserve energy are investigated. Some of the solutions that were considered are as follows:

4.1.1 Ganging of levels in the upstream

Ganging of levels can be done in the upstream to increase the number of nodes participating in the upstream and hence increase the PDR. Two types of ganging are considered: dual-level and triple-level. When a node in DL^{n-1} transmits using W_n, any node that can D&F at W_n will repeat at W_{n-1}, if it has not repeated the message before and if it is identified with (1) DL^n or DL^{n-1} for dual-level ganging and (2) DL^n, DL^{n-1} or DL^{n-2} for

triple level ganging. Even though these two schemes increase the node participation and PDR when the upstream source is not too far from the sink, it has been shown in Chapter 5 that they are not effective when the source is far away. Since this is not a viable solution, the single-level OLACRA described in the earlier chapter is used for all the future simulations/ protocol variations.

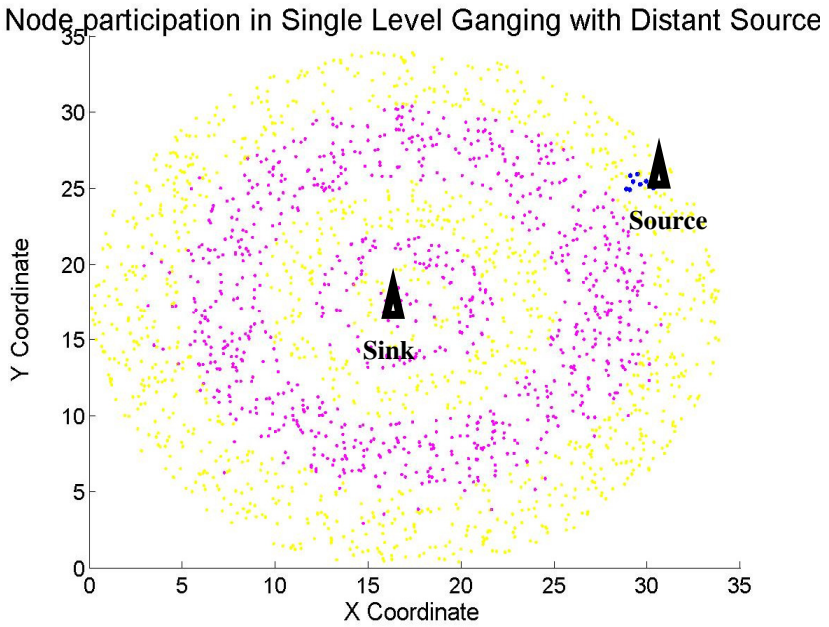

Figure 3: Node participation in single-level OLACRA with distant source.

4.1.2 Increase the power of the source node for the upstream transmission.

While effective, this approach is not practical because any node could be a source, therefore all nodes would require the expensive capability of higher power transmission.

4.1.3 OLA-T flooding in just the first upstream level

This scheme allows all nodes in DL^n that can decode a message to forward the message

if they have not forwarded that message before until an OLA meets the upstream forward boundary of DL^n. Two variations of flooding are explored in this section.

4.1.3.1 OLACRA with Flooding and Threshold (OLACRA-FT)

The worst case number of broadcast OLAs required to meet the upstream forward boundary of DL^n can be known a priori as a function of the downstream level index. For example, in Figure 4(a), three upstream broadcast OLAs are needed to meet the upstream forward boundary of DL^n. The union of the upstream decoding nodes (e.g. all three shaded areas in Figure 4(a)) in DL^n), are then considered an "extended source." To save energy, the nodes in the extended source that transmitted in the downstream transmission are commanded to not transmit in the extended source transmission; in other words, those nodes that were near the forward boundary in the downstream would be near the rear boundary in the upstream, and therefore will not make a significant contribution in forming the next upstream OLA. Next, the extended source behaves as if it were a single source node in an OLACRA upstream transmission; this means that all the nodes in the extended source repeat the message together, and this collective transmission uses the same preamble, as would a source node under the OLACRA protocol. In order for the nodes to know when it is time to transmit as an extended source, an OLA waveform distinction (different preamble bit), similar to the network initialization phase of OLACRA, must be used in this upstream flooding phase. Figure 5(a) shows an illustration of the node participation in OLACRA-FT.

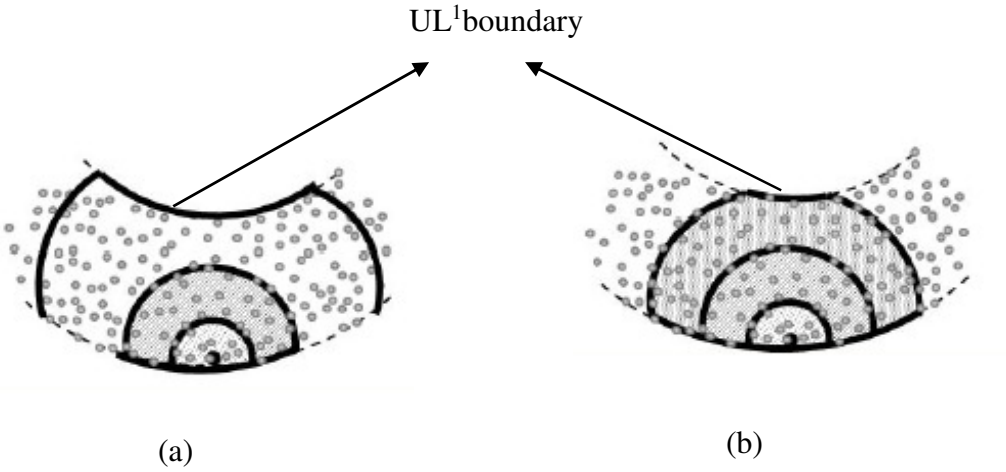

Figure 4: UL[1] flooding to improve PDR in (a) OLACRA-FT and (b) OLACRA-VFT.

4.1.3.2 OLACRA-FT with variable relay power (OLACRA-VFT)

The energy-efficiency of OLACRA-FT can be enhanced by optimizing the relay powers of the initial flood levels in the upstream. Consider the case in Figure 4(a) where the boundary of the third OLA flood level is just before the downstream rear boundary of DL^{n-1}. Here the DL^{n-1} upstream source node would do an OLA flood for three levels, as required by OLACRA-FT making the width of the extended source really large, thereby making the scheme energy inefficient. The skinniest strip width, which corresponds to the largest energy savings, is obtained when the boundary of the last OLA upstream flood level is just above the downstream rear boundary of DL^{n-1} as in Figure 4(b). Since the radius depends on the relay power, this can be achieved by varying the relay power on the initial flooding stages, P_{rf}, to have the last upstream OLA flood boundary be as close to the downstream rear boundary of DL^{n-1} as possible. Similar results can be obtained by varying the transmission threshold, τ_f, or a combination of both.

While both methods, varying transmission threshold and varying relay power in the

flooding level, try to vary the radii of the flood levels, they achieve it in different ways. While reducing relay power increases the number of levels required to reach DL^{n-1}, thereby making more number of nodes transmit at a lower power, decreasing the transmission threshold decreases the number of nodes transmitting but the transmission is at a higher power. OLACRA-VFT has been simulated in this thesis by optimizing the relay power of the flood levels, P_{rf}. Note that the transmission threshold for the initial OLA flooding stages is fixed in this case and that only nodes in these flooding stages transmit using the optimized relay power, P_{rf}. The downstream OLA levels and OLACRA levels in upstream use relay power P_r as defined in earlier sections.

4.1.4 OLACRA with Step-size Control (OLACRA-SC)

As will be shown in Chapter 5, OLACRA-FT and OLACRA-VFT have high reliability (high PDR), but their energy efficiency is low as they make large number of nodes participate in the transmission as shown in Figure 5(a). Hence another alternative to enhance upstream connectivity is investigated. OLACRA-SC simply aims to reduce the downlink step-size, so that there are enough nodes in UL^2 to carry on the transmission. The downlink radii depend on the downlink transmission threshold and relay power [13]. Thus step-sizes in the downlink can be controlled by optimizing the transmission threshold or relay power on the downlink to have smaller fixed downlink step-sizes. Unlike OLACRA-FT and OLACRA-VFT, the goal here is not to reach the downlink reverse boundary, but to fire enough nodes in UL^2 to carry the transmission back to the sink. This can be observed in Figure 5(b). ‘

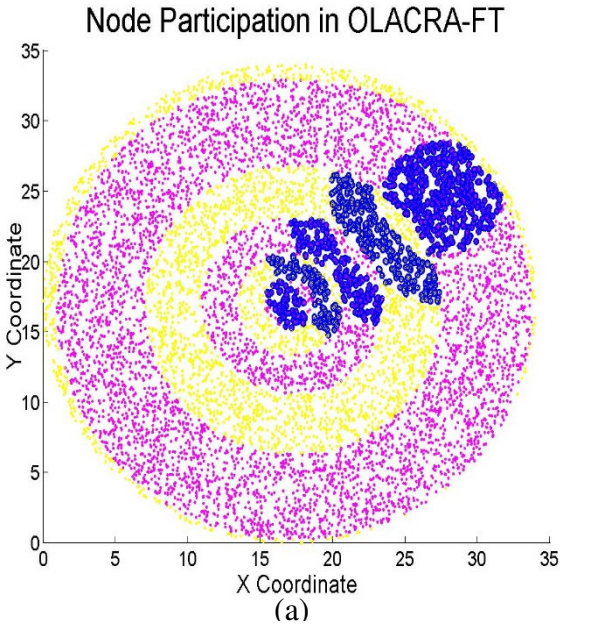

(a)

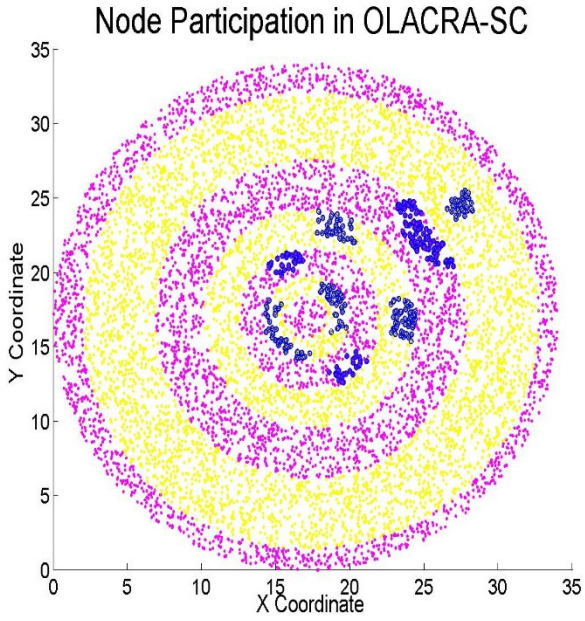

(b)

Figure 5: Node participation in (a) OLACRA-FT and (b) OLACRA-SC.

To further increase the energy savings, only the nodes that participated in the downlink OLA-T are allowed to relay the message in the upstream. This is in contrast to OLACRA-FT where energy was saved in the extended source by commanding the nodes that did not

relay in the downlink OLA-T to transmit in the upstream. Even though the scheme in OLACRA-FT is more energy-efficient, it is not possible in OLACRA-SC as there is a high possibility that the nodes that relayed in OLA-T would not be taking part in the upstream OLACRA-SC transmission. This is the case in Figure 5(b).

4.2 EFFECT OF NODE DENSITY ON UPSTREAM CONNECTIVITY

Because the number and placement of the nodes is random, there is a chance that there might not be enough nodes in the vicinity of the source to form an OLA when the node density is low. If this happens, there are no relays, and the packet will not be delivered. This problem is called "initial bottleneck."

A little analysis of this initial bottleneck can be performed. Let A be the event that there are no nodes within the decoding range of the source, and let B be the event that the message fails to get to the sink. Then $A \subseteq B$ and $P(A) \leq P(B)$. It is straightforward to calculate $P(A)$.

The hypothesis is that even with all the enhancement schemes described above, like OLACRA-FT, OLACRA-VFT and OLACRA-SC, the probability of outage cannot be less that $P(A)$. One of the solutions to this problem is to use a higher source power for just the upstream source node. However this has the disadvantages mentioned in 4.1.2. An alternative way to decrease the probability of outage due to initial bottleneck is to explore retransmission diversity schemes [29]. However this is beyond the scope of this thesis. $P(A)$ will be evaluated in Chapter 5.

CHAPTER 5

PERFORMANCE RESULTS: OLACRA

Closed-form analytical results are difficult to obtain for the upstream using OLACRA and its variations because of the generally irregular shapes of the upstream OLAs. Hence, Monte Carlo simulation is done to demonstrate the validity and explore the properties of the OLACRA protocol. First, the variations of OLACRA are evaluated over the deterministic channel, with step-size control considered separately. Next, the diversity channel is considered followed by some examples of practical parameter values that correspond to the normalized values used in simulations.

5.1 DETERMINISTIC CHANNELS

Each Monte Carlo trial has nodes randomly distributed in a circular area of radius 17 with sink located at the center. For all results in this section, $\tau_d = 1$ and 400 Monte Carlo trials are performed. The downstream levels are established using OLA-T with source power $P_s = 3$, relay power $P_r = 0.5$.

5.1.1 Without Step-size Control

A node density of 2.2 is considered in these simulations. A fixed RTT of 4 is used for the downstream.

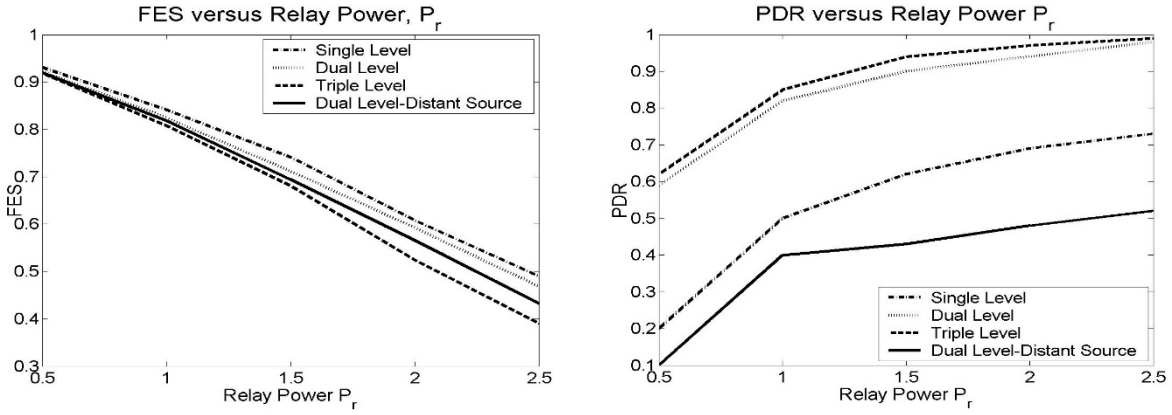

(a) (b)

Figure 6: (a) FES and (b) PDR versus relay power for different variants of OLACRA.

Figures 6(a) and 6(b) compare different versions of OLACRA in terms of FES and PDR versus the relay power. The upstream source node is located at a radius of 15 for the dual-level distant source (DLDS) case, and at a radius of 5 for the other cases. These two cases are considered to show the variations of FES and PDR with distance from the sink. Single-level case has the highest FES for all values of relay power; however the PDR is very low. Dual-level and triple-level have higher PDRs, with only a small degradation of the FES relative to single level. Though the FES value of dual level when the source is close to the sink was comparable to dual level distant source (DLDS) case, the PDR is very low for DLDS. The reason is that the distant source is in a downstream level so thick that the dual level upstream ganging is not enough to reach the upstream forward boundary.

Figures 7(a) and (b) compare the performances of the different variants of OLACRA in terms of their FES and PDR versus RTT in dB. The upstream source node is located at a radius of 15. Relay power of 1 is assumed for upstream routing. The relay power for the flooding stage in OLACRA-VFT P_{rf} is 0.6. OLACRA-T with a source power of 1 has the highest FES of 0.87 at RTT of 1.76 dB; however the PDR at this RTT

is very low = 0.12. The FES of OLACRA-FT is lower than OLACRA-T with source power = 1, but the PDR for this case is very high. A further improvement in FES of OLACRA-FT is obtained with OLACRA-VFT. OLACRA-T with a source power of 6 performs similarly to OLACRA-FT, which shows that the upstream source power requirement will be very high to achieve similar performance.

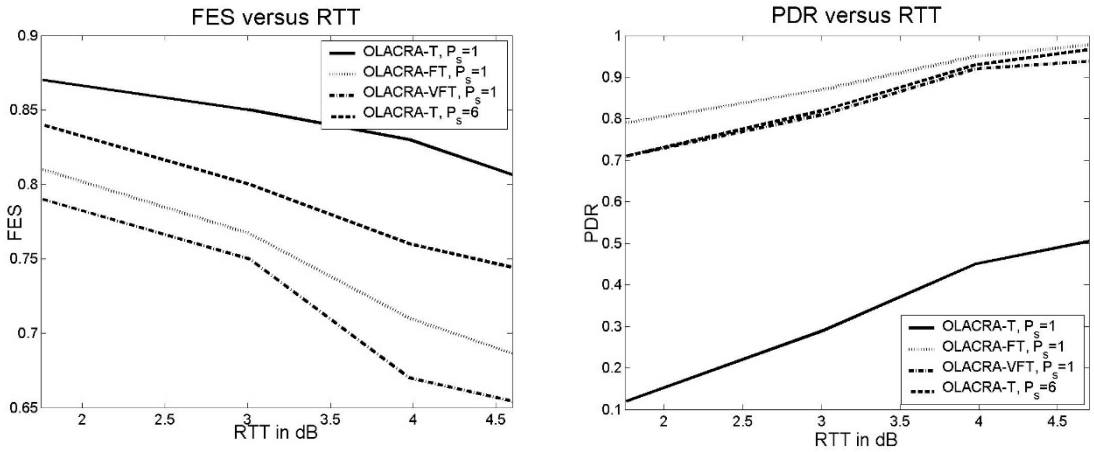

(a) (b)

Figure 7: (a) FES and (b) PDR versus RTT for different versions of OLACRA.

5.1.2 With Step-Size Control (OLACRA-SC)

For the results in this section, a much higher density of 10 is considered, keeping $\bar{P}_r$ constant at 1. The RTT values in the downlink are designed to obtain fixed downlink step-sizes using the continuum approach. Two step-sizes are considered: $0.8rd1$ and $rd1$, where $rd1$ denotes the first downlink radius.

Figures 8(a) and (b) compare the FES and PDR performances of $0.8rd1$ and $rd1$. The $0.8rd1$ has a very high FES of 0.928 at a RTT of 1.76 dB, however the PDR at this RTT is very low. This is because of the low value of RTT. A lower value of RTT suppresses

a large number of nodes thereby reducing the PDR. This effect is more pronounced in the fixed step-size case compared to the general OLACRA, because the small step-size alone prevents a large number of nodes from participation. Use of RTT removes a substantial amount of nodes from a set that already did not have many nodes to begin with. As RTT is increased to 4.5 dB, the PDR for *0.8rd1* improved to 0.927.

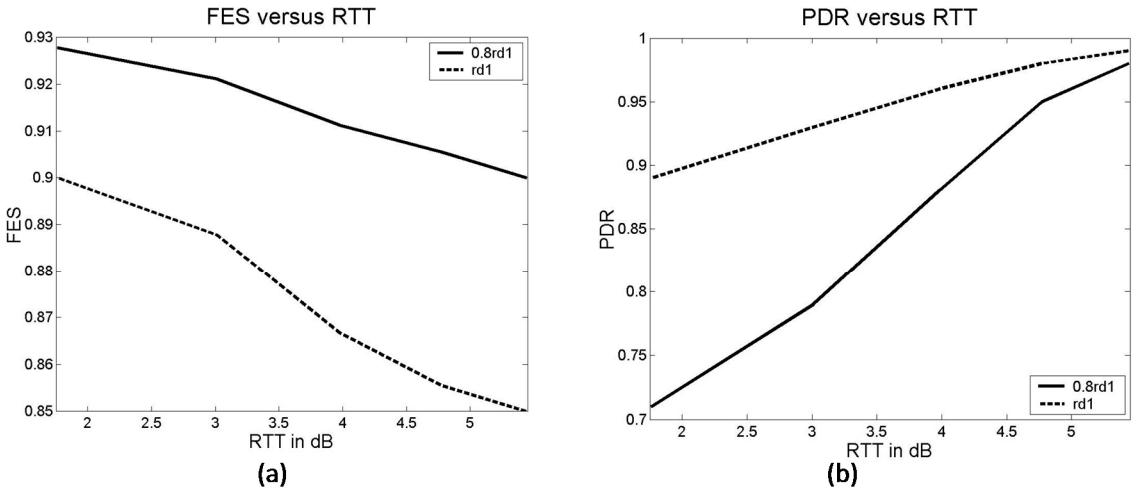

Figure 8: (a) FES and (b) PDR versus RTT for OLACRA-SC.

Compared to the $0.8rd1$ case, the $rd1$ case has a lower FES and a higher PDR. But even the FES for the $rd1$ case is much higher than the FES observed for a general OLACRA or OLACRA-FT.

Figure 9 shows the variation of FES with distance from the sink. Step-size optimization is done for the downlink with fixed step-sizes of $0.8rd1$ and all other parameters are chosen as in the previous result. Even though the step-sizes follow the continuum-predicted fixed values very closely at smaller radii, they tend to stray away more at higher radii. This can be seen as the larger step-sizes with increase in radii in Figure

9 (wider saw-tooth with increasing distance from the sink in Figure 9). This is because even though the continuum tool is valid at very high densities, the validity of continuum prediction falls at lower densities.

It can be seen that the FES decreases as the distance of the source from the sink increases. This is very intuitive, as more nodes have to take part when the source is at a greater distance from the sink. It can be seen that FES has a saw- tooth variation within a level. Within a level, the highest FES was observed close to downlink forward boundary. This was because when the upstream source is at this location, minimum numbers of nodes are activated in the next upstream level, whereas when the upstream source node is closer to the downlink forward boundary it activates maximum number of nodes in the next upstream level. The sharp saw-tooth fall of FES happens because of the change in level of the node. That is a node at 1.414 is a part of downstream level 1 and hence is one hop away from the sink, whereas a node at 1.414 is in downstream level 2 and is two hops away and hence activates much more nodes.

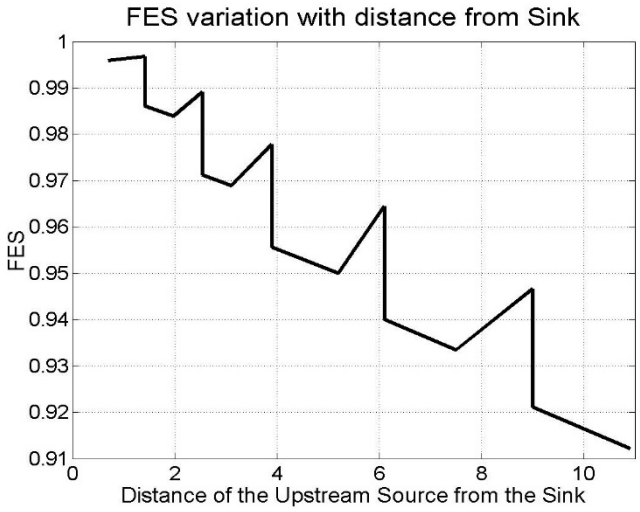

Figure 9: FES versus distance of the upstream source node from the sink.

5.2 DIVERSITY CHANNELS

Each trial has 2000 nodes uniformly and randomly distributed in a circular field of radius 17. The downstream levels are established using OLA-T with source power $P_s = 3$, relay power $P_r = 0.5$ and RTT of 4. For upstream routing using OLACRA, the source node is located at a radius 13 with $P_s = 1$. A decoding threshold of 1 is chosen for the downlink and the uplink transmissions. A relay power of 1 is used for the upstream levels. The relays transmit direct sequence spread-spectrum (DSSS) waveforms and choose their transmission times from a window m chips long. The chip time, T_c, of the DSSS signal is 500 time units. A rake receiver with m fingers is present at the receiver to extract the diversity.

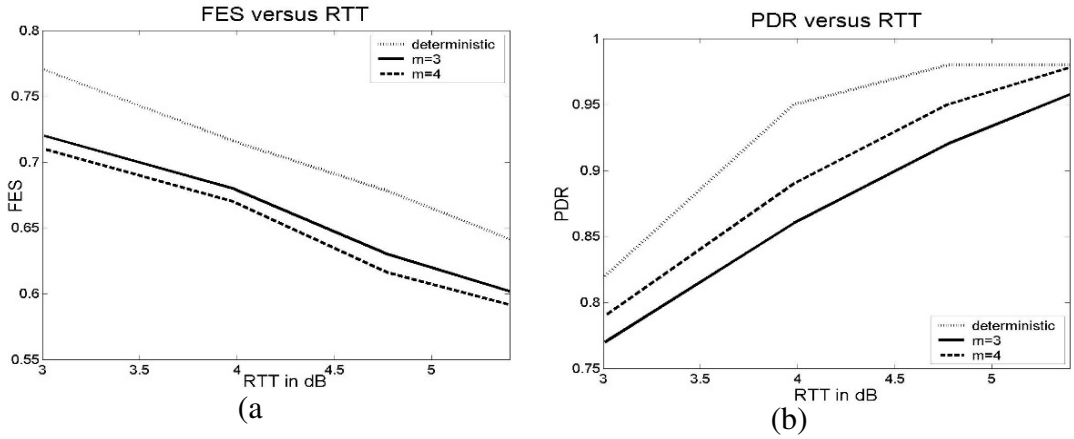

(a) (b)

Figure 10: (a) FES and (b) PDR versus RTT for the diversity channel model.

Figure 10(a) compares the FES under OLACRA under the deterministic channel model and diversity channel model, for different values of RTT, while Figure 10(b) shows the PDR, also versus RTT. For m = 3 (third order diversity) FES is 0.72 at RTT = 3 dB, whereas the FES for the deterministic case for the same value of RTT is 0.77. Similarly the

probability of message delivery at the sink is only 0.77 for the m = 3 case at RTT of 3 dB, whereas the probability of success for the deterministic case is higher at 0.82 for the same RTT.

But when the diversity order was 4 (m = 4), the performance characteristics of the fading channel got closer to the deterministic case. For m = 4 the probability is about 0.94 for an RTT of 4.7 dB, when the deterministic case has a probability of 0.97. It should also be noted that the FES performance of m = 4 case is not very different from the m = 3 case, meaning that the higher probability of message reception obtained by having an additional rake finger is not at the cost of energy.

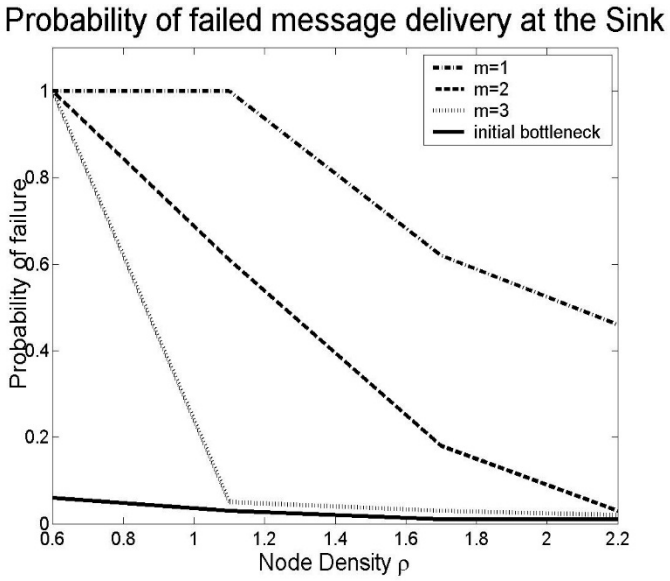

Figure 11. PDR versus node density.

Figure 11 captures the variation of the probability that the message is not decoded by the sink versus node density ρ for different values of m (diversity order). The curve labeled "initial bottleneck" shows the probability that there are no nodes in the first level

in UL^1 . At m = 1, which corresponds to the "no diversity case," the probability of failure is 1 for $\rho < 1.15$, Even at a much higher density, $\rho = 2$, the probability of failure drops only to 0.54. That it drops with increasing density is consistent with the claim in [5] regarding non-orthogonal transmissions. However when m = 2, the probability of failure tends to zero at a node density of 2.2. When m = 3, probability of failure drops to 0.01 at a node density of 1.1. It should be observed that the m = 3 and "initial bottleneck" lines are very close for $\rho \geq 1.1$, implying that at m = 3, the probability of failure is dominated by the probability that there are no nodes in the first level ("initial bottleneck") since the probability of outage due to fading tends to zero.

Figure 12 shows the received power distribution of a node located in UL^3 at a radius of 7 m. The three vertical lines correspond to the power received at each of the orthogonal dimensions (rake fingers in this case). It is observed that the total received power at each of the rake fingers converges to about 2, thereby giving full "third order diversity." Thus it can be inferred that by intentionally delaying the source transmissions the channel can be orthogonalized into m orthogonal flat-fading channels with equal power.

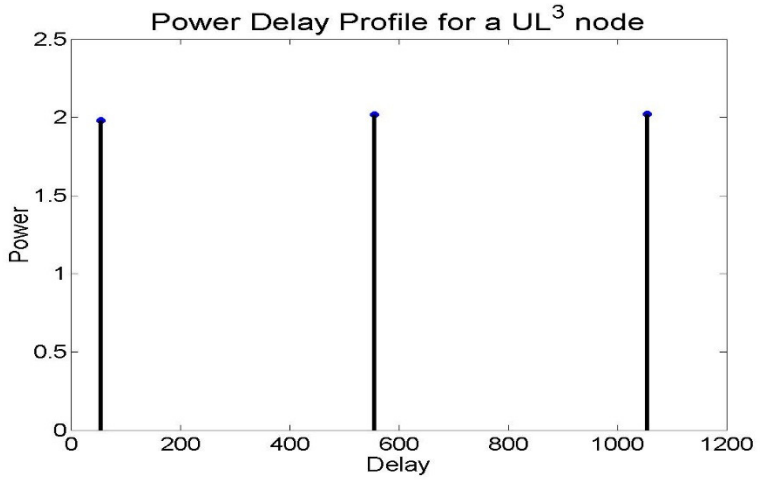

Figure 12: Power delay profile for OLACRA.

5.3 EXAMPLES OF UNNORMALIZED VARIABLES (PRACTICAL SCENARIOS)

The results given so far have been in terms of normalized units. This section presents some examples of un-normalized values for these variables to give an idea of what power levels and node densities can achieve the performance shown in the above results. A similar table was presented in [13]. The table in this thesis gives more examples that better fit the cases considered in this thesis. Most of the results in the simulations assume a DR of 1. Expanding the decoding ratio (DR) in terms of un-normalized values,

$$DR = \frac{\text{Re}\,ceiver\ Sensitivity}{\frac{P_t G_t G_r}{d_0^2}\left(\frac{\lambda}{4\Pi}\right)^2\left(\frac{Number\ of\ Nodes}{Area\ in\ m^2}\right)d_o^2} \quad . \tag{8}$$

Suppose the radio frequency is 2.4 GHz ($\lambda = 0.125m$), and the antennas are isotropic ($G_t = G_r = 1$), then (8) can be simplified to

$$DR = \frac{\text{Re}\,ceiver\ \ Sensitivity * 10^4}{P_t\ in\ mW\left(\frac{Number\ of\ Nodes}{Area\ in\ m^2}\right)} \quad . \tag{9}$$

Table 1 shows five different examples of un-normalized variables and their resulting d_{nn} and DR values obtained using (9). A DR of 1 is used for most of the results in Chapter 5. DR = 1 can be obtained in Examples 1, 2, 3, and 4, ranging from high density (2.2 nodes/m^2) to low density (1 node/5 m^2). The high-density cases, Examples 1 and 2 correspond to very low transmit powers.

Table 1: Examples of un-normalized variables

Example	P_t (dBm)	Node Density	RX sensitivity (dBm)	DR
1	-50.00	1 nodes/ m^2	-90.00	1.0
2	-50.00	2.2 nodes/ m^2	-86.57	1.0
3	-57.00	1 node/ 5 m^2	-90.00	1.0
4	-43.98	1 node/4 m^2	-90.00	1.0
5	-20.97	9 node/3.60 km^2	-90.00	0.5

CHAPTER 6

OLA ROUTING ON DEMAND (OLAROAD)

OLAROAD is an OLA-based reactive routing protocol suitable for MANETs. A MANET is a self-configuring network of mobile wireless nodes, in an arbitrary topology with no existing infrastructure. Because of node mobility, the topology changes rapidly and hence MANETs require reactive routing protocols, which compute routes on the fly. Reactive routing protocols like Ad hoc On-Demand Distance Vector (AODV) routing [30] and Dynamic Source Routing (DSR) [31] have been shown to be appropriate for mobile environments, because they cope quickly with topological changes.

The objective of CT-based unicast routing, is to determine a series of node clusters between the source and the destination. Most of the existing CT-based ad hoc routing protocols assume that a conventional multi-hop route already exists or that clusters have somehow already been defined [22, 23, 24, 25]. However, approaches that require a pre-existing route lead to additional overhead in MANETs. More recently, opportunistic CT-based routing schemes have also been proposed [32, 33, 34], where the actual forwarding cooperators are not pre-determined, but decided on the fly, based on signal strength measurements, NACK signals and assigned priorities. However [32] assumes an existing multi-hop route, and [33, 34] must identify a list of potential cooperators before the actual transmission begins. None of these schemes will avoid the high levels of complexity, overhead, and delay required to do multi-hop routing in mobile networks.

CT-based routes that do not require that the cooperators are part of a multi-hop route are several nodes wide and are more like a strip or “river” of nodes through a network.

Without a pre-existing multi-hop route, other means are required to define the cooperating nodes. One previous work proposes using location information to define the boundaries [26]. However, some MANET applications might not have location information. Also, to reduce the computational load, designers may wish to avoid using the coordinates for route computation, even if the coordinates are available. In contrast, the proposed OLAROAD scheme avoids these scalability problems, because no nodes are individually addressed (aside from the source and destination nodes), and the complexity of the proposed scheme is independent of node density, given the density is high enough to support OLA transmission [4]. Also, there is no centralized control and no coordination between pairs of individual relay nodes. In other words, the proposed scheme requires no explicit medium access control (MAC) function for a single flow; collisions from multiple simultaneously transmitting nodes are exploited to attain an SNR advantage through diversity combining [4]. That an OLA, or "virtual array," occupies an area rather than a single point is one reason why OLA-based routing is tolerant of limited node motion. Another distinction is that in OLAROAD, CT is incorporated in both the route set-up and data transmission phases, whereas in all existing schemes, cooperation is done only in the data transmission phase.

This section compares AODV to OLAROAD for a mobile network. It is shown that as density increases, with node degree (average number of nodes in the decoding range of the transmitter) held constant, the AODV routes require a larger number of route refreshes. This is because as the density increases, the number of hops in the route also increases, and hence the probability that the route breaks due to mobility also increases. In contrast, the OLA-based cooperative route is invariant to changes in density and the route stays "fresh"

longer in a mobile network because an OLA is defined over an area instead of at a point. Additionally the end-to-end delays of the two protocols are compared. It is shown that the end-to-end delay in OLAROAD is lower because of two reasons: less delay caused by route refreshes, and fewer hops in the cooperative route compared to the multi-hop route.

The results in this chapter are limited to networks with a single flow and single packet transmission per flow. Even though this assumption greatly abstracts behavior of many networks, it gives very useful insights on the operation of OLA flows and how they compare with AODV flows. Extensions to multiple packets and multiple packets per flow are done in later chapters.

6.1 DESCRIPTION OF OLAROAD PROTOCOL

Like the existing reactive routing protocols, such as AODV and DSR, OLAROAD involves mainly three phases: (1) Route request (RREQ) broadcast by the source node (2) Route reply (RREP) unicast by destination node and (3) Unicast data transmission (DATA). As mentioned earlier, the RREQ and RREP phases are done using OLACRA-SC. OLACRA-SC brings cooperative diversity to both route discovery and data transmission without requiring any centralized control and requires no individual addressing of relay nodes. Please note that OLACRA-SC has been modified slightly, as will be explained below, to suit the OLAROAD scheme.

6.1.1 RREQ (Forward Path Set-up)

The source node initiates a broadcast route discovery process by broadcasting using OLA-T (first phase of OLACRA-SC) a RREQ message when it needs to communicate

with another node for which it has no routing information. The RREQ message format is given below.

< *source address, broadcast ID, destination address, downlink level number, DATA, Uplink/Downlink bit* >

Like conventional AODV, the pair <*source address, broadcast ID*> uniquely identifies a RREQ, and the *broadcast ID* is incremented whenever a source node issues a new RREQ. The *DATA* bit distinguishes the DATA and RREQ transmissions. The *Uplink/Downlink bit* is appended to the message to indicate the direction of flow. A node relays a message only if it has not previously relayed a message with the same *broadcast ID* and *source address,* and while relaying it increments the *downlink level number*. The levels form concentric rings as shown by the dotted circles in Figure 13. The details of the OLA-T algorithm have been given in detail in Volume 1.

Like the traditional AODV, every relay node keeps track of the information in the RREQ message in order to implement the reverse path setup, as well as the forward path set-up that will accompany the transmission of the eventual RREP.

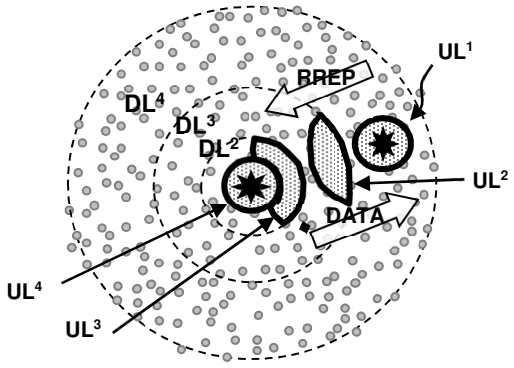

Figure 13: RREQ, RREP and DATA phases in the OLAROAD scheme.

6.1.2 RREP (Reverse Path Set-up)

The Phase II of the routing algorithm is the reverse path set-up, which is initiated by the destination node when it receives the RREQ and has sufficient resources to carry out the transmission. This is the same as the Phase II (upstream phase) of the OLACRA-SC algorithm, which has been explained in Volume 1. A RREP has the same fields as the RREQ. The thick solid curves in Figure 13 enclose the upstream decoding levels, and the arrow labeled "RREP" shows the direction of the RREP message.

6.1.3 DATA Transmission

The union of the uplink *decoding* levels defines the *cooperative route*. As soon as the source node decodes the RREP, it starts the DATA transmission through this cooperative route. In other words, the DATA flows through the same decoding levels illustrated in Figure 13 for the RREP, but in the direction indicated by the arrow labeled "DATA." Please note that cooperative route is defined by a set of nodes and not by an actual boundary. All the nodes in this cooperative route that can decode the DATA are eligible to relay DATA if they have not relayed it before.

In mobile networks, the cooperative route becomes wider and sparser with time because of the random motion of the nodes. A transmission threshold makes this route even sparser as it further limits node participation. Therefore, to provide more robustness against mobility, no transmission threshold is used for the DATA phase.

OLAROAD shares many features with the traditional AODV. Like AODV, OLAROAD is also a reactive scheme, which does not require the source node to transmit the whole route along with the DATA (i.e., not a source-routing scheme). A transmitting

OLA in OLAROAD is analogous to a relay node in AODV, in that they both only remember their immediate neighbors for the particular source-destination pair. As in AODV, the immediate neighbors are established using the *backward* and *forward pointers* that are formed in the RREQ and RREP phase as described earlier. OLAROAD also shares the lower overhead of the AODV scheme, but is more reliable than the latter because of the benefits of cooperative transmission.

6.2 PERFORMANCE RESULTS

Monte Carlo simulation is done to explore the properties of the OLAROAD protocol. A square field of dimension 100 m X 100 m is considered. WE consider a single flow, and single packet transmission per flow for this section. The source node is located at coordinates (50 m, 50 m) and the destination node is located at (10 m, 90 m). The receiver sensitivity is –90 dBm. G_t and G_r are taken to be 1 and the frequency of transmission is 2.4 GHz.

When OLAROAD and AODV are compared, the node density will be the same, but the relay power will be 10 dB lower for OLAROAD than for AODV, such that AODV's node degree is 31.4 while OLAROAD's node degree will be 3.14. This is done in an effort to make the per-hop total transmit powers of the two protocols *roughly* equal. It should be noted that if the node degree for AODV is reduced to be more comparable to that of OLAROAD (by reducing AODV transmit power), AODV's performance would be significantly degraded because many more hops would be needed in the route.

The RTT values for the RREQ phase have been chosen as in [35] to give a fixed step-size of *0.8rd1* in the downlink, where *rd1* is the radius of the first downlink level. For

the RREP phase, a fixed RTT of 1.76 dB is used, whereas no RTT restriction is imposed on the DATA transmission phase.

For modeling mobility, the Random Way Point (RWP) mobility model is used [31]. Nodes randomly choose their speed from an interval (0-5 m/s). The pause time, T_{pause}, is taken to be zero.

In order to find the packet delivery ratio (PDR) in a multi-hop network, a new function called the "connectivity function" is defined. This function is taken to be zero when there is no route between the source and destination nodes, and is one when there is a route between the source and destination nodes. The ensemble average of the connectivity function over 100 trials is obtained at every time instant to obtain the PDR as a function of time. It is noted that this way of finding PDR is slightly different from the conventional definition, which is a time average. In this work the PDR is found as an ensemble average instead of a time average so that the dynamics can be revealed.

Two densities and sets of transmit powers are considered in this simulation. For $\rho = 0.1$ nodes/m^2, 1000 nodes are distributed randomly in the square field. The transmit power P_t of the source and relay nodes is –30 dBm for AODV and –40 dBm for OLAROAD, and these powers are used for all the three phases of the protocols. For $\rho = 1$ nodes/m^2, 10,000 nodes are considered and the transmit power is –40 dBm for AODV and –50 dBm for OLAROAD, and these powers are used for all the three phases of the protocols.

Figure 14 demonstrates how PDR varies with time and node density. The PDR curves for the AODV cases have a saw-tooth variation. The peaks of the saw-tooth correspond to the times immediately after a route discovery, and the troughs correspond to

the times with the least connectivity. As time and density increase, the route refresh times in AODV become more random and vary more with trials, which is the reason for diminishing differences between peaks and troughs.

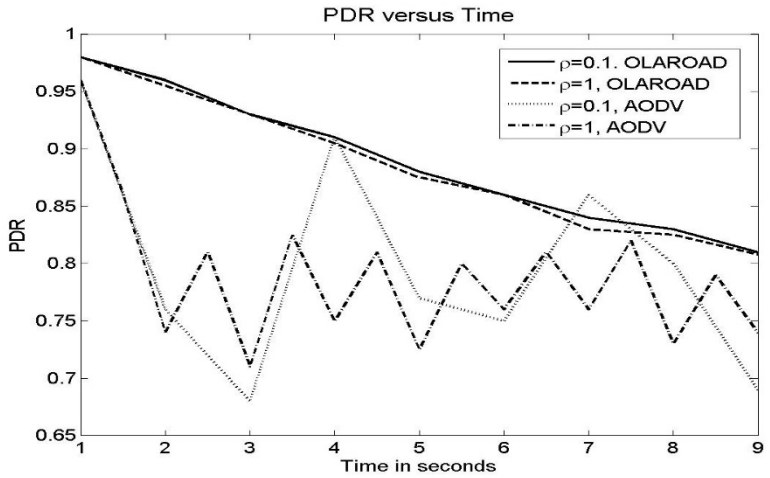

Figure 14: PDR versus time for the AODV and OLAROAD schemes.

It can be seen that the PDR of OLAROAD is independent of the node density, whereas AODV requires more route refreshes (and hence additional overhead and delay) as the density increases. This is because at higher densities nodes transmit at lower power (to keep the node degree constant), and hence the AODV route from the source to the destination has larger number of shorter-length hops. If any one of these hops fails, the route fails, so the probability of failure of the route increases with the number of hops. In contrast, the number of hops in OLAROAD is determined by the node degree and stays the same in both the densities considered.

In Table 2 the variation of aggregate relative latency (ARL), which is defined as the ratio of the end-to-end delay for OLAROAD scheme to the end-to-end delay for

AODV, for different power levels is shown. The DATA transmission is at the power levels listed in Table 2. The RREQ and RREP phases are done at –30 dBm for AODV and –40 dBm for OLAROAD in both cases.

For calculating the end-to-end delay, the data transmission time after the cooperative route is formed and also the time for route refreshes and route discoveries after the route breaks is considered. It can be seen that even though OLAROAD uses a lower transmit power per node it requires less time to reach the destination node. For obtaining results in this table, the simulation is for 15 seconds and the end-to-end delay for each packet is calculated and the time average is computed. The ratio of the time average of the end-to-end delay for both of the schemes gives ARL. It is also observed that as the nodes start transmitting at higher relay powers, the end-to-end delay benefit of OLAROAD decreases in comparison with AODV.

Table 2: ARL for different P_t (ρ=0.1).

P_t (AODV) (dBm)	P_t (OLAROAD) (dBm)	ARL
-30	-40	0.712
-20	-30	0.822

CHAPTER 7

CONTENTION REGION ANALYSIS FOR OLA UNICAST NETWORKS

While the previous chapters compared cooperative transmission with classical point-to-point schemes, they were conducted in a setting with a *single packet* transmission through a network limited to a *single source*, several relays and a destination. However, networks generally operate with multiple packets and multiple flows, where each nodes' transmission is affected by the transmissions happening at its neighboring nodes'. This is because a wireless nodes transmissions' consumes bandwidth shared with other nodes in the vicinity since these nodes cannot simultaneously access the shared medium. More specifically, wireless transmissions consume bandwidth at all nodes within the carrier-sensing distance of the transmitting node. In addition to contention between different flows (called *inter-flow contention*), multiple nodes along the same multihop path (forwarding the same packet) maybe located within the carrier-sensing range of each other and prevent multiple transmissions. This in turn leads to *intra-flow contention* i.e., contention between packets belonging to a single flow that are forwarded at different hops along a multihop path and *intra-OLA contention*, i.e., contention between packets belonging to the same hop in the same flow that are forwarded at slightly different times. Intra-flow, Interflow, and Intra-OLA contentions have significant effect on the throughput, delay and other performance metrics, and we will show that ignoring these interferences will lead to network performance overestimation of over 4 times.

In order to make a fair comparison of bandwidth utilization/ spatial reuse of a OLA flow and a non-CT flow, both the number of nodes suppressed and the time for which they

get suppressed should be taken in to consideration. This is because, even though OLA transmissions have larger suppression regions compared to non-CT routes, they finish faster. This is because the hops are longer and so fewer hops are required to get from the Source to the Destination. Hence it is not fair to compare the Bandwidth utilization of OLA and non-CT multihop just based on their suppression regions (number of nodes suppressed that delay their transmission because of carrier sensing). Hence we devise two metrics (a) Contention Count, to account for the number of nodes that get suppressed, and (b) Suppression Time, to account for the time they get suppressed for to compare the flows.

The main contributions of this chapter are as follows: The first section of this chapter defines in detail the two performance metrics that will be used in this chapter. Later, the OLA hops and their suppression regions are carefully studied; we show that suppression regions in the uplink are hop dependent and asymmetric, and the width of the uplink OLAs (*step-width*), and hence their corresponding suppression regions increases with uplink index. The suppression region variation with hops and a comparison with a non-cooperative multihop scheme are presented. This is the first work that studies the suppression regions of uplink OLAs with a realistic network model, and compares it with a non-CT network. Based on our analysis, a contention-aware MAC layer modification to OLACRA-SC called Hop-Optimized OLA (HOOLA) is proposed. Lastly, the performances of the different OLA unicast schemes (OLACRA-SC and HOOLA) and the challenges in using a traditional CSMA-based MAC scheme for OLAs are identified.

7.1 DEFINITIONS AND PERFORMANCE METRICS

7.1.1 Contention Count

To quantify the effects of intra-flow and interflow interference from an OLA transmission (or a node in a multihop non-CT route), it is important to know the *contention count* [36] at each router (which is a node in the non-CT route, or an OLA in the OLA route). The contention count (CC) at a node/hop is the number of nodes that are located within carrier-sensing range of the given node/ hop. Contention count has a significant impact on the bandwidth consumed by the flow. The *effective bandwidth* consumed by a flow at each router is the CC times the single hop flow bandwidth requested by the application. Hence, determination of the CC is an important parameter in comparing the Bandwidth Utilization of different routing protocols.

The problem of contention-count aware routing has been studied extensively in earlier works for multihop non-cooperative networks [36, 37]. The focus of these works has been to find the contention count in a distributed fashion, and to incorporate the contention count in the routing metric. The optimization in these works was in the routing layer where the objective was to select the route that had the least contention count. Our optimization, on the other hand, is on the MAC layer, where given a route we investigate methods to reduce its contention count by optimally selecting the cooperators.

7.1.2 Suppression Time

Even though the longer hops in OLA unicast routes result in larger contention counts compared to a multihop non-CT route, they also result in a shorter time to get to the Destination (as there are fewer number of hops). So even though a large number of nodes

will be suppressed, they will be suppressed for a shorter time compared to a multihop non-CT route. Because of this significant difference, it isn't fair to compare the Bandwidth Utilization just based on Contention Count. Hence, to take in to account the lower transmission time of OLA routes, we devise a new metric called *Suppression Time*. Suppression Time of a hop/ route is defined as the total number of nodes suppressed in that hop/ route multiplied by the time for which they are suppressed. It should be noted that, unlike Contention Count, suppression time is very much dependent on the packet size, wireless channel, Data Link Layer/ MAC Design etc. (For example, as the packet size goes up, routes which have fewer number of hops to the Destination will have a better suppression time than routes with larger number of short hops).

7.2 CHALLENGES IN SUPPRESSION REGION OPTIMIZATION FOR OLAS

In this section, we study the problem of suppression region optimization and explain why it is more challenging compared to both non-CT multihop networks, and OLA broadcast networks.

7.2.1 Step-width growth of Uplink OLAs

While the issue in the OLA downlink was the growth of the step-sizes, the issue in the uplink is the growth of the step-width. This can be seen in Figure 15, which shows a simulation plot of OLACRA-SC with no DR applied in the uplink. As can be seen, the width of the uplink OLAs increase with their index. This happens due to the following reasons: (1) The first few OLAs in the unicast route have a lower decoding threshold compared to the final levels to ensure connectivity. Hence, using the same decoding

threshold (and not a decreasing one) for all levels in OLACRA-SC increases node participation with index. (2) The higher number of nodes transmiting in an OLA will result in a longer transmission range; this results in the receiving OLA from getting wider, as the step-size is limited by the downlink level boundaries. The range of an OLA is directly proportional to the width of the transmitting OLAs, hence the width keeps increasing with index.

Step-width, unlike step-size in downlink, cannot be controlled easily with DR, or transmit power. This is because reducing the transmit power/ or increasing DR to reduce the step- width would also result in suppressing the uplink boundary nodes, which are the most critical in maintaining packet reliability. Hence, steps should be taken to ensure reliability while performing step-width reduction.

7.2.2 Asymmetric Contention Regions of OLAs

Another challenging problem for suppression region optimization in the OLA uplink is the asymmetric and hop-dependent contention regions of the OLA hops. (A link from node N1 to N2 is said to be asymmetric, if node N1 can decode N2's transmission, but node N2 cannot decode N1's transmission).

Consider again Figure 15, the dotted line shows the boundary of UL6's suppression region. As can be seen, the transmission from nodes in UL6 might suppress nodes even in UL2. However, the suppression region of UL2 is much smaller. On comparison, in multihop non-CT route, the suppression regions of all nodes in the route are similar and circular. Because of these asymmetries, the suppression region reduction schemes should

be hop dependent. In addition to suppression region optimization, asymmetric links make the design of MAC layer schemes for OLA very hard, as will be shown in the next chapter.

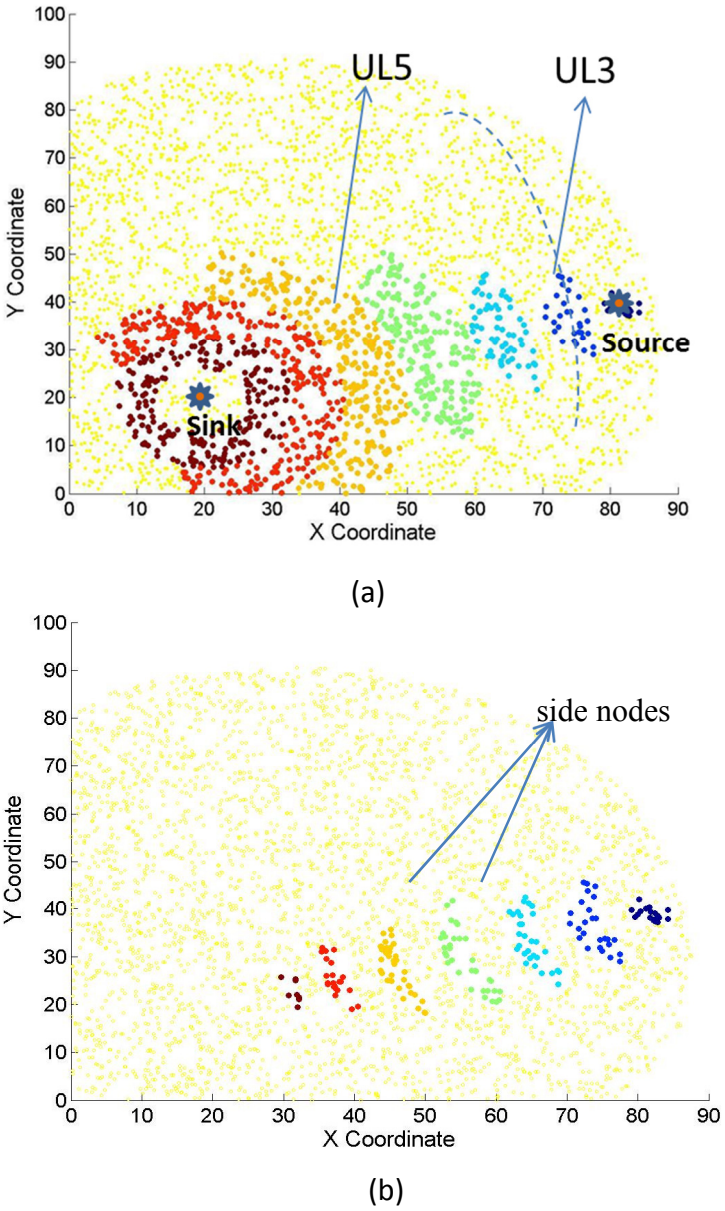

Figure 15: Simulation plot for (a) OLACRA-SC, (b) HOLA – threshold

Asymmetries can occur in multihop non-CT routes too when the nodes transmit at different transmit powers, or have asymmetric channels between them. However, the

asymmetry in OLA networks is caused in large part by the asymmetric node participation, and hence occurs even when all nodes transmit at the same power, and have the same wireless channel characteristics. However, unlike step-width increase, asymmetric contention region is a challenge in both OLA uplink and downlink. The problem however is more manageable in the downlink as the downlink levels are deterministic and hence easier to optimize.

7.2.3 Unpredictable/ Irregular Contention Region Shapes

For non-cooperative networks with isotropic antennas, the area suppressed by each of the nodes in the route is almost a circle, which is directly dependent on the transmit power of the node. Hence suppression regions can be changed by varying the transmit power; the nodes could be commanded to transmit at the minimum power required to maintain connectivity thereby minimizing the contention count. On comparison, OLA suppression regions are irregular, and don't have a direct relationship with the transmit power. Two OLA hops with the same total transmit power could have entirely different suppression regions. This is because, in addition to the transmit power, the coverage area of an OLA depends on the locations of the cooperating transmitters. The cooperators are not handpicked, but created on the fly, hence their locations are not known in advance. It depends on the locations of the nodes in the previous OLA, which in turn depends on its previous OLA. Because of this it is hard to control the suppression region of an OLA or predict the minimum transmit power required to maintain connectivity in an OLA. Hence transmissions might usually be at a higher power, resulting in bigger suppression regions. It should be noted that the suppression regions of OLAs would also change when nodes

move around, whereas the suppression regions of a node in a non-CT route don't change with mobility or other topology variations.

7.3 UPLINK OPTIMIZATION FOR IMPROVING BANDWIDTH UTILIZATION

As we have seen in the last section, the suppression regions and their optimizations are harder in uplink OLAs compared to non-CT networks due to the step-width increase, and asymmetric and unpredictable contention regions of OLAs. However, it should be noted that the asymmetry and unpredictability of OLA is caused mainly by the step-width increase. Schemes that reduce the step-size, will also partly address the asymmetry and unpredictability of uplink OLAs. Hence in this chapter, we specifically look at the causes of step-width increase. Based on this, we propose an optimization called Hop-Optimized OLACRA (HOLA). HOLA and some of his variants are described here.

7.3.1 Causes of Step-Width Increase

7.3.1.1 Curvier OLAs

For all the CT/ non-CT multihop schemes that have been proposed so far, the shapes of the receiving hop/ node is determined by the location (s) and transmit power (s) of the transmitting hop/ node. However, in OLA unicast flows, in addition to the location and power, the boundaries of the downlink levels limit the height and thereby determine the shape of the uplink OLAs formed. As it can be seen in Figure 15, while UL1 is a circle, UL3 can be approximated by a square. However as the uplink OLA index increases, the OLA boundaries become more curved (concavity in the direction of Source increases). As the curvier OLA has a higher effective range in the direction towards the Source. However,

the increases range presents itself as a increased step-width as the height of the OLA is limited by the downlink boundary. Hence the step-width increases with increasing index.

7.3.1.2 Wider OLAs

Another property of upstream OLAs is that they get wider as they get closer to the Source. A wider OLA will have a longer effective range, as shown in [5]. Again, as the step-size is limited by the downlink boundaries, this results in the step-width increasing further. So a wider OLA results in an even wider OLA.

One of the reasons for the step-size increase in OLACRA-SC is the use of same transmission threshold for all levels. A higher threshold is required in the initial levels to maintain connectivity; however reusing the same threshold in later levels results in step-width increase. The wider OLAs don't increase the effective range, as the range of the OLA is limited by the downlink boundary. Also, it is hard to limit the width of OLAs using boundary node conditions. This is because such conditions will also limit the useful nodes and thereby affect the transmission success.

7.3.2 Hop- Optimized OLACRA (HOLA)

In this scheme, instead of fixed step-sizes, the downlink step-size optimization is done such that the step-size of the downlink OLA is decided by how many hops away it is from the Source. That is the decoding threshold for a level increases with its index. By doing this, we prevent the step-width growth in the uplink, and the asymmetries and large contention regions caused by that. This variation is called the Hop-Optimized OLACRA (HOLA). For example, UL1 would have a lower decoding threshold in comparison with UL6. Since the

uplink OLAs get curvier and wider as they get closer to the Sink, the hop distance will be longer. We consider two variations of HOLA:

(a) HOLA-threshold: In HOLA-threshold the longer range of the final uplink OLAs is limited by using a higher threshold

(b) HOLA-power: To exploit the longer range of the final uplink levels, the step-size of the initial downlink levels are optimized. This would result in shorter number of hops in the uplink. However, this would result in asymmetric contention regions, and hence is applied only in initial downlink levels.

Figure 15 (b) shows a simulation plot of HOLA-power. It can be seen that the node participation (and thereby contention regions) has been greatly reduced in comparison with OLACRA-SC. However it should be noted that HOLA is not a fully optimized solution. To understand this better, consider the "side nodes" shown in the figure. These nodes are farthest from the destination OLA and hence their contribution is minimal. However, due to their side location, their contribution to interference is maximum. Unlike the downlink, it is harder to suppress these side nodes using a transmit power (Decoding Ratio) criteria. The transmit powers of the side nodes would be just "barely above the threshold", hence suppressing them would also suppress the nodes that contribute the most to the next level and reduce reliability.

Figure 16 shows the suppression regions of a HOLA flow and a non-CT multihop flow (This is just an example simulation plot and a more detailed comparison of the suppression regions will be done in the next section). The pink dots represent the nodes that are

suppressed in OLA routing, and the blue dots represent the nodes that are suppressed in non-CT routing.

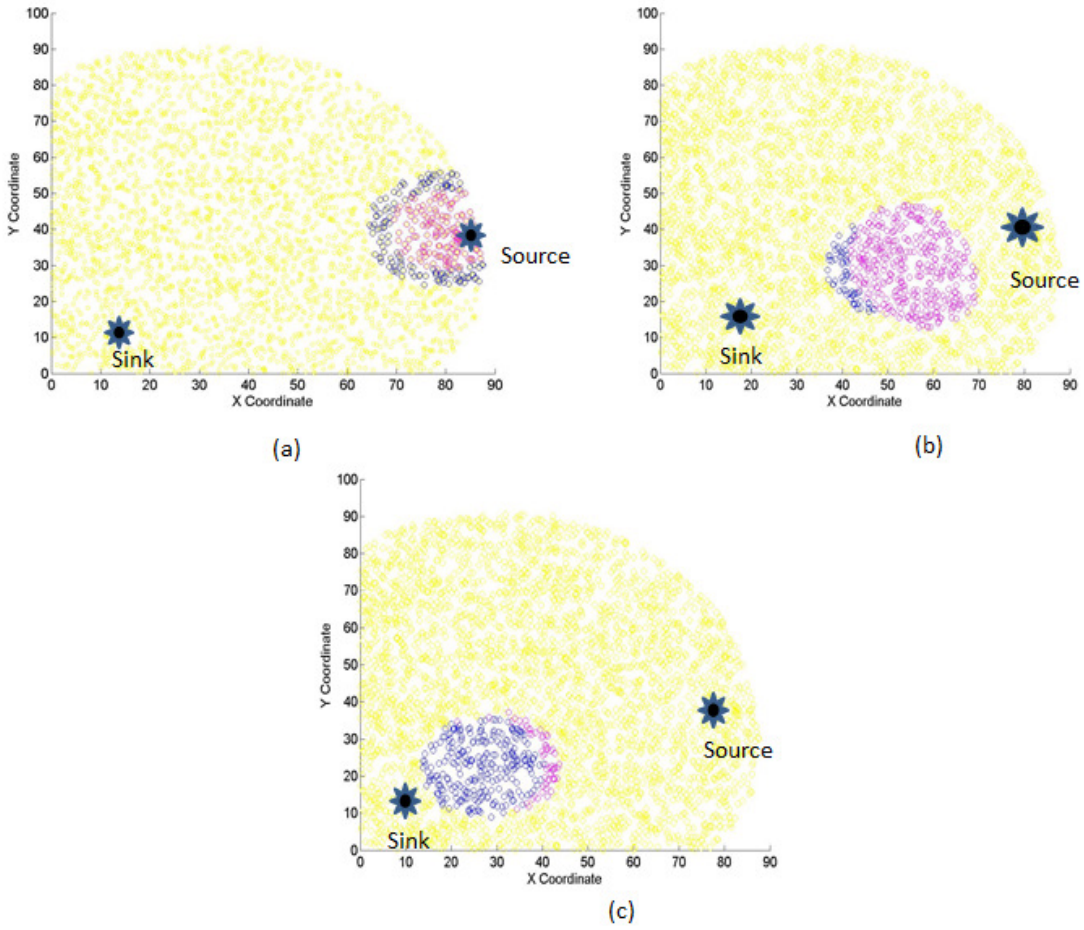

Figure 16: Contention Region comparison for OLA (pink) and Multihop Route (blue) for (a) first hop (b) middle hop, and (c) end hop

The OLA and non-CT flows are chosen such that the total number of hops from the Source to Destination are same for both schemes. Figure 16 (a) compares the suppression regions of the first uplink hops of OLA and non-CT scheme, Figure 16 (b) compares for a middle hop and Figure 16 (c) compares for an end hop (last but one hop). It can be seen

that the while the suppression regions of the non-CT scheme is almost circular, the suppression region sizes and shapes are hop-dependent. For the first level, the suppression region is larger for non-CT compared to OLA, while for the middle hop, the OLA suppression region is much bigger. For the end hop, it's seen that the OLA suppression region is similar to the non-CT suppression region. This figure is just a simulation plot, a more detailed analysis of the suppression region variations and their causes will be done in Section 8.3.

7.4 PERFORMANCE RESULTS

In this section, we analyze the contention counts and suppression times for each of the OLACRA-SC and HOLA schemes, and compare them with those of a non-CT multi-hop scheme.

Each Monte Carlo trial has 5000 static nodes randomly distributed in an area of dimension 100 m X 100 m. The Sink is located at (20 m, 20m) and the upstream source node is located at (80 m, 20m). Receiver Sensitivity of -90 dBm and a carrier sensing threshold of -100 dBm are assumed. Data rate of 250 kbps, and packet size of 128 bytes is used for the simulation (based on the IEEE 802.15.4 standard). An inter-packet spacing of 13 ms is used (which is approximately 3 times the packet duration, and is a common assumption in ad hoc networks). Downstream levels are established using OLA-T with source power P_s = -57 dBm. Step-size optimization is done in the downlink to obtain downlink levels with fixed step-sizes. The DR values used in the downlink are as in Chapter 5 for OLACRA-SC and HOLA-threshold. For the uplink transmission, transmission powers are chosen such that the total number of hops from the Source to the Destination is

the same for OLACRA and the non-CT scheme. The source and relays transmit at -40 dBm in the non-CT scheme. The source power is -43 dBm and the relay transmit power is -50 dBm for the OLA schemes.

For the Data Link Layer, channel reservation using CSMA with RTS/ CTS handshake is implemented for both OLA and multi-hop non-CT schemes. Every node in an OLA, before transmitting the packet, checks if the physical medium is busy. If it is not busy, it sends a short RTS packet of 60 bytes to its destination (we don't consider intra-OLA contention in these results, i.e., if a node senses another transmission of the same packet by another node in the same OLA, it ignores that and transmits the packet). A node in the receiving OLA that decodes the RTS, sends a CTS of 60 bytes in response to the RTS. Only the nodes in the transmitting OLA that receive the CTS will transmit the DATA packet after sensing the channel. Unlike the traditional RTS/CTS exchange, a retry is not initiated by nodes that do not receive the CTS after transmitting the RTS.

In the first of the following sections, we present a comparison of the Contention Count, and Suppression Time of OLA-based unicast schemes (OLACRA-SC, HOLA-power and HOLA-threshold) and non-CT shortest hop multihop scheme. Dependence of contention region on OLA hops is also presented. Later, we investigate (1) the effect of step-size optimization on the end-to-end reliability, and (2) study the effectiveness of RTS/ CTS-based CSMA for OLA unicast transmissions.

7.4.1 Contention Region Comparison for OLA and Non-CT Multihop Flows

Figure 17 compares the Contention Count Ratio (CCR) of HOLA- Threshold, HOLA-Power and OLACRA-SC (Decoding Ratio = 1 for Uplink). It can be seen that the CCR

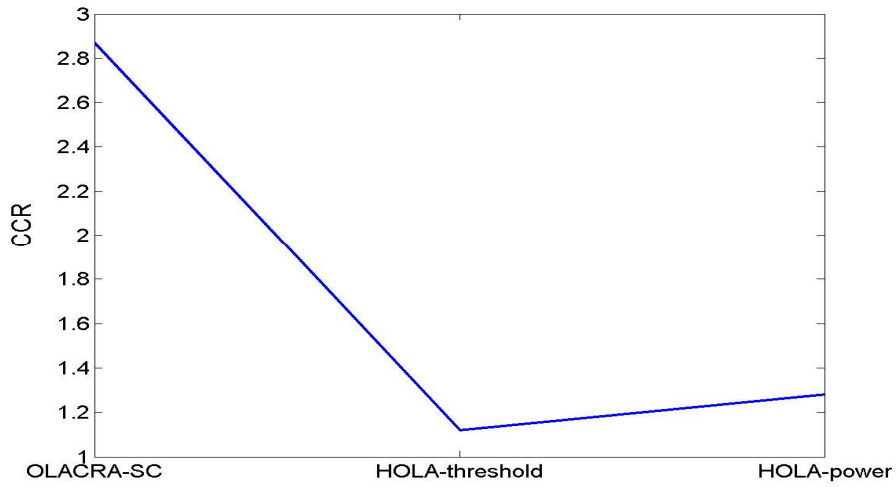

Figure 17: Contention Count Ratio for different OLA Topologies.

reduces from 2.8 for OLACRA-SC to 1.1 for HOLA-threshold, showing that the hop-based optimization in the upstream significantly improves the Bandwidth utilization. The CCR for HOLA-threshold and HOLA-power are similar to the multihop non-CT scheme, meaning that they suppress similar number of nodes in the upstream. The CCR for HOLA-power is slightly greater than HOLA-power. This is because the uplink levels closer to the Sink in HOLA-threshold are bigger compared to HOLA-threshold, and hence have bigger suppression regions. It should be noted that we don't count the nodes participating in transmission towards the contention count. HOLA exploits a portion of the already suppressed nodes to relay the message, thereby reducing the transmit power requirement on each node, and making the communication more robust.

To understand the suppression regions better, and see how the CCR varies between different levels, Figure 18 investigates the hop by hop suppression region of OLA hops. The CCR for all the OLA schemes is 0.5 for the first upstream level, it increases till the 5th

upstream level, then starts decreasing. This can be explained as follows: The Source transmission (for first level) is non-cooperative for OLA schemes, and hence the CCR depends only on the relative transmit powers of OLA schemes (-43 dBm) and non-CT scheme (-40 dBm). Since the OLA transmission is at a lower power, it suppresses less

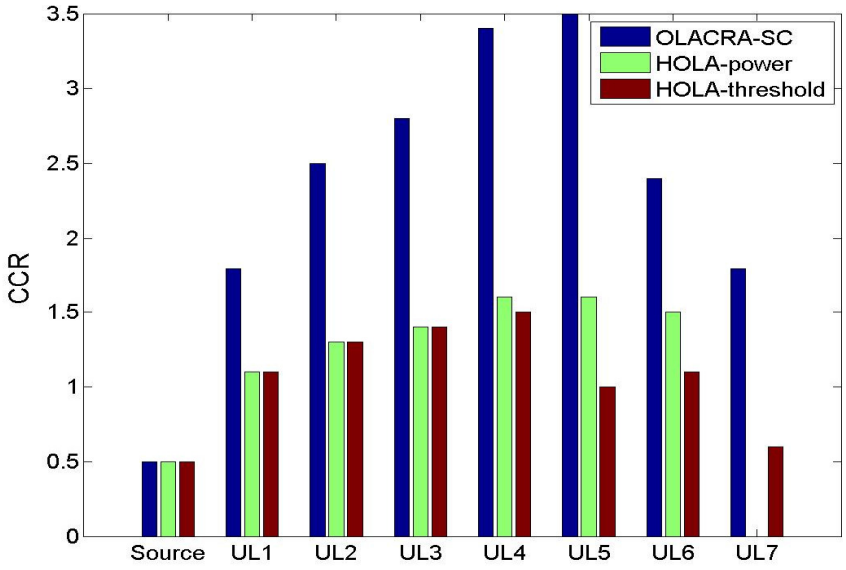

Figure 18: CCR per level for OLA Unicast protocols

number of nodes. After the first level the OLA hops are cooperative transmissions and hence have larger contention counts. However, the CCR starts decreasing after the 5th level; this is an artifact of the OLA downlink levels. The areas of downlink levels are smaller as they get closer to the Sink. Hence the number of nodes that participate in transmission goes down and hence the contention count too. It should be noted that the CCR for HOLA-threshold and HOLA-power is much less than OLACRA-SC for all levels showing that hop-level optimization can significantly reduce suppression regions. After the 4th UL,

HOLA-power suppresses more nodes compared to HOLA-power. This is because HOLA-power employs a lower decoding threshold compared to HOLA-threshold in UL4 and beyond. Because of the lower decoding threshold, HOLA-threshold has a longer range, and hence gets to the Sink in just 6 hops. This is why HOLA-power doesn't suppress any nodes in the 7th level.

Figure 19 compares the Suppression Times of OLACRA-SC, HOLA-power and HOLA-threshold with the multihop non-CT scheme. The suppression time ratio's (STR) of HOLA-power is similar to its CCR. This is expected as they have the same number of hops and similar suppression areas. The Suppression Time for OLACRA-SC is very high compared to the HOLA schemes and the multihop non-CT scheme. This is because there are a large number of unsuccessful RTS and CTS messages due to the asymmetric link sizes. HOLA-power has a better suppression time because of two reasons: (1) it has fewer number of hops so the nodes are suppressed for a shorter time (2) the overlap region is less, resulting in lower Suppression time.

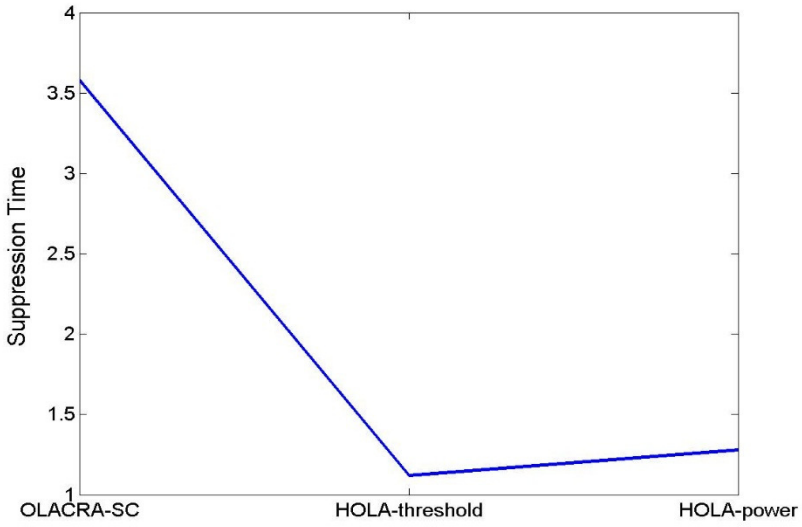

Figure 19: Suppression Time Ratios for different OLA Topologies

7.3.2 RTS/ CTS Effectiveness for OLA Unicast Flows

Figure 20 compares the Packet Delivery Ratio (PDR) for the different OLA unicast schemes. The objective of this experiment was to (1) understand the effect of contention region optimization on the end-to-end reliability of transmission, and (2) understand how effective a traditional RTS/CTS-based CSMA for OLA networks was. Unlike the previous chapters, PDR is calculated as a time and ensemble average, where the averaging is performed over 100 packets and 100 trials. It is seen that the PDR of OLACRA-SC (with CSMA MAC with RTS/ CTS handshake) is very low at 0.37, which is in direct contrast with results from Chapter 7, where the PDR of OLACRA-SC was over 0.9. This is because the PDR was calculated earlier as an ensemble average for a single packet; hence it didn't take into account packet losses due to intra-flow contention and asymmetric links.

For OLA unicast flows with asymmetric OLAs, nodes in a smaller OLA could be under the suppression region of nodes from a larger OLA, but not the other way. For such cases, a RTS or CTS by the smaller OLA doesn't reserve the channel, as the nodes in the larger OLA will not hear it resulting in packet loss. This is why the PDR is very low at 0.37 for OLACRA-SC.

On the other hand, the HOLA-based schemes have reliability over 0.8. Thus it can be inferred that hop-based step-size optimization, reduces asymmetry of the uplink OLAs, and significant improves reliability. However the reliability of HOLA with RTS/ CTS is less than HOLA with CSMA. This is unexpected as traditionally RTS/ CTS have been

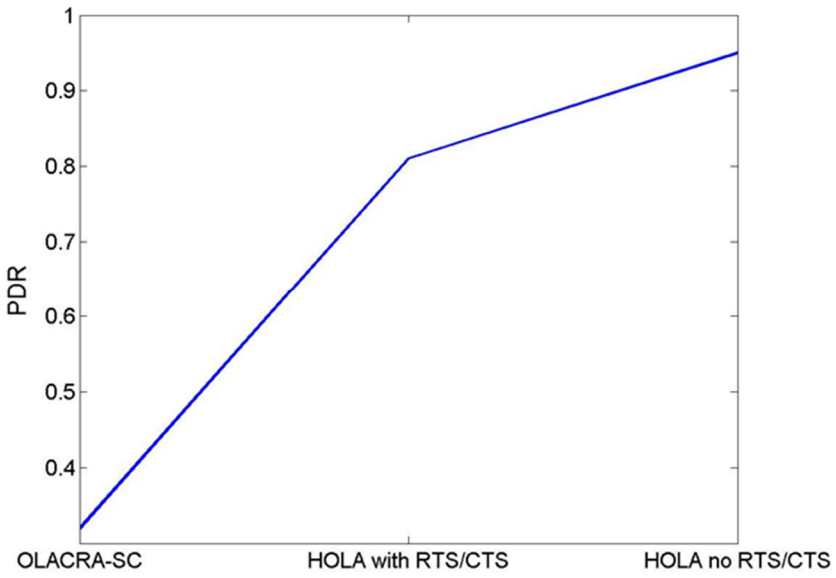

Figure 20: Packet Delivery Ratio for different OLA Topologies/ MAC Designs.

shown to increase the end-to-end reliability in both non-CT multihop and multihop schemes. The reason for this is that the links in HOLA are not perfectly bidirectional (even with step-size control and hop-based optimization). A portion of nodes in a transmitting OLA might not hear the CTS from the receiving OLA, because of the asymmetry of links. These nodes (which were required in making transmission successful) would not take part in the DATA transmission and hence brings down the reliability. Thus it can be seen that a RTS/CTS-based data link schemes which is widely used in 802.x networks, cannot be used in OLA networks. Instead of improving reliability, it suppresses required nodes and decreases the reliability of transmission. This shows the need for designing data link layer schemes specifically suited for OLA flows.

CHAPTER 8

DATA LINK LAYER DESIGN FOR OLA UNICAST FLOWS

In the previous chapters, the objective was to compare the reliability and bandwidth utilization of OLA unicast flows relative to non-cooperative unicast transmission. It was assumed that the flows had CSMA/ CA with a RTS/ CTS handshake. However, the OLA flows have very different properties from non-cooperative flows, and simply applying the CSMA-CA architecture would not be efficient. As we saw in Figure 18 in Chapter 7, an RTS/ CTS mechanism would decrease the reliability of transmission, as it limits some critical nodes from transmitting. In this section, we carefully examine the challenges in designing a data link layer for OLA flows, the issues in using a RTS/ CTS/ ACK – based CSMA scheme in OLA unicast flows, and propose extensions to the CSMA with RTS/CTS/ACK handshakes that would work in OLA networks. We will show that some of the properties of OLA routing, including no individual node addressing, and no centralized control, which make them very useful in distributed ad hoc networks, make the design of their MAC/ Network layers very challenging. Based on our study, we propose a Cluster Head-based MAC scheme and Survivability Mechanism for OLA routing. We compare the performance of OLA flows with a new MAC with the traditional scheme AODV.

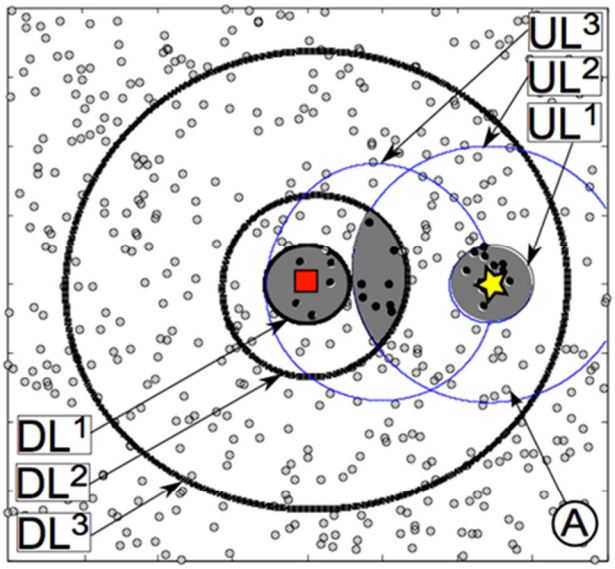

Figure 21: OLAROAD Figure

8.1 CHALLENGES IN DATA LINK LAYER DESIGN FOR OLA FLOWS

8.1.1 Non-addressability of OLA nodes

One of the reasons why OLA routing has low overhead is that no nodes are individually addressed. However this makes the data link layer design more complicated. The following example shows an instance where a traditional RTS/CTS/DATA/ACK handshaking CSMA/ CA protocol is not suitable for OLA unicast flows. In Figure 21, if UL1 sends an RTS to UL2, and UL2 sends back its CTS, a portion of nodes in UL1 wouldn't receive the CTS because of the link asymmetry. These nodes wouldn't transmit, making the DATA transmission from UL1 to UL2 weaker. This was shown in Figure 20 in Chapter 7. Similarly, if UL2 sends back an ACK to UL1, some nodes that transmitted DATA won't receive the ACK. However, the transmission is successful, because, there are "sufficient" nodes in each level that take the transmission forward. So even if an ACK is not received, it doesn't mean that the transmission was not successful. From this example,

we can see that RTS/ CTS/ ACK messages cannot be directly extended to OLA-networks. In both examples, a portion of nodes in an OLA receive some message, and a portion does not. There is no one node which is responsible for making a decision on the transmission success. So a retransmission protocol is problematic.

In contrast, for non-OLA CT networks, a conventional non-CT route is formed before the cooperators are recruited and the nodes in the conventional route are responsible for confirming the receipt of a CTS or ACK. The problem is challenging in OLA routes because there is no conventional route or cluster head that can be made responsible for receiving ACK or CTS.

Even though step-shape optimizations have been considered in the last chapter to make the OLAs symmetric, it is hard to ensure *perfect bidirectionality* (every node in UL1 can hear the UL2 transmission, and every node in UL2 can hear the UL1 transmission). Hence there would be situations where nodes within the same OLA make a different decision on a transmission success/ failure.

8.1.2 Asymmetric Contention Regions due to Diverse OLA Shapes

The second challenge in OLA MAC Design, as explained in Chapter 7, stems from the asymmetric contention regions of OLAs, specifically when OLAs have different shapes. For example, in Figure 22, consider UL^2, which is the second upstream OLA in the first flow (grey color), and UL^1-2 which is the first upstream OLA of the second flow (blue color). UL^2 is a circular uniform OLA and has an almost circular contention region, bounded by the blue dotted circle. UL^1-2 has an asymmetric contention region, which is longer in the vertical direction and smaller in the horizontal direction. As can be seen, UL^1-

2 falls under the contention region of UL^2 , whereas UL^2 does not fall under the contention region of UL^1-2. This is happening because the shapes of the contention regions are different (even if they have the same number of nodes in the OLA and same total transmit power, the shape of the suppression areas would be different). In this case, UL^2 might start transmitting while UL1-2 is transmitting/ receiving causing collision at UL^1-2. On comparison, non-CT networks have similar contention regions if they are using the same power, and hence if Node A is in Node B's contention region, Node B would be in Node A's contention region as well. When situations like this happen, the OLA Data Link Layer should be able to detect this change, and wait/ re-route (or grow the OLA)/ transmit as required to maintain connectivity.

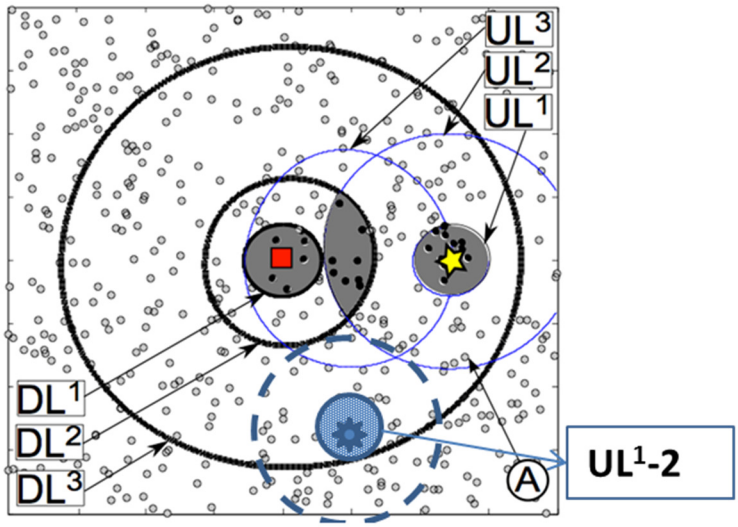

Figure 22: OLAROAD Figure

8.2 DATA LINK LAYER DESIGN FOR OLA UNICAST FLOWS: PROTOCOLS

To overcome the challenges/ differences mentioned in the last section, a new Data Link Layer is designed for OLA networks. The Data Link Layer Design for OLA Unicast Networks has two parts. A *Cluster-Head-based handshaking* that is used for channel

reservation and ensuring success of DATA transmissions in an OLA network, and an *OLA Size Adaptation Mechanism*, that finds alternate robust links in case of link failures, both transient and permanent.

8.2.1 Cluster Head (CH)-based Handshaking

As we saw in Section 8.1, one of the challenges in using RTS/CTS/DATA/ACK based handshaking in OLA is that there is no node in an OLA that is responsible for ensuring the control messages are received. This is challenging especially when there are conflicting reports on the receipt of a message within the same OLA.

To circumvent this issue, we propose to have a Cluster Head (CH) in each OLA, which is responsible for the following

(1) ensuring a CTS is received after sending RTS, and communicating the receipt of CTS within its OLA

(2) ACK is received after sending the DATA, and communicate the receipt of ACK within its OLA.

(3) Initiating a retry of RTS/ DATA when the CTS/ ACK is not received.

(4) Initiating OLA Size Adaptation Mechanism, when a link failure is detected.

8.2.1.1 Cluster Head Selection scheme

Ideally the CH should poll each of the nodes in the OLA to see their report on the receipt of the CTS/ ACK and intelligently fuse the inputs and make a decision on whether the CTS/ ACK were received. Since cluster head selection and distributed decision making has been extensively studied in the context of sensor networks, we don't consider CH/ data

fusion optimization techniques in this work. Instead we use a simple scheme described below to select the Cluster Head. The Data Link Layer design could be made more robust by adopting a more optimal CH selection scheme.

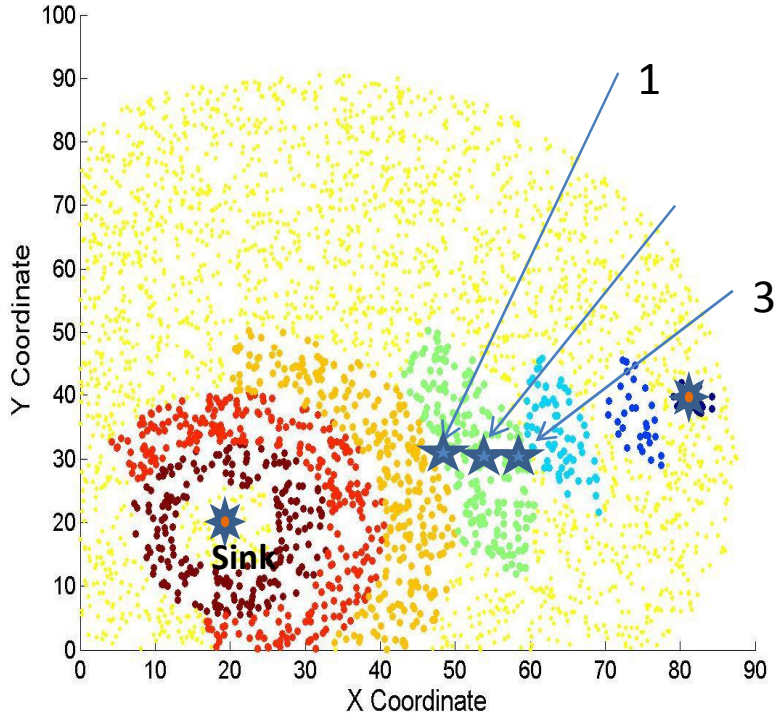

Figure 23: Cluster Head Location Comparison

8.2.1.2 Location of Cluster Head

The location of the CH within an OLA is very important in determining how effective it is. For example, if the CH is in "1" in Figure 23, is a very optimistic selection, as the CH would receive the CTS/ACK even when majority of nodes don't and make an incorrect decision. "3"n 3 is a very pessimistic assumption as the CH won't receive the CTS/ACK even when majority of the nodes in the OLA have received and the transmission is

successful. Hence we conclude that "2", which is a centrally placed location within an OLA, puts the CH in a position where it can make an accurate estimate of the reception of CTS.

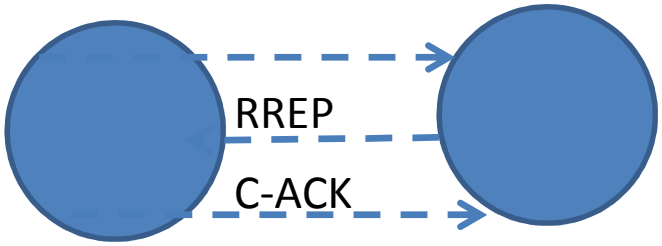

Figure 24: Cluster Head Selection Mechanism

8.2.1.3 Simple Cluster Head Selection Method

The Cluster Head Selection Process in OLAROAD is shown in Figure 24. During the RREP phase, every node in UL^{n} will make a note of its received power from UL^{n-1}. When the source receives the RREP message, it will send another small control message called C-ACK to the Destination. The purpose of this message is to aid the nodes in an OLA to determine the received power from ULn+1, and thereby to select the best Cluster Head. On receipt of the C-ACK, nodes in ULn will make a note of the received power from ULn+1. After this phase, nodes in ULn will have the received power values from both its transmitting and receiving OLA. The CH is selected based on the following design.

Let $P_{i,n+1,}$ be the received power at i^{th} node from UL^{n+1}, and $P_{i,n-1}$ be the received power from UL^{n-1}. A node is selected as the CH if it meets the following criteria

$P_{i,n+1} > \tau_{CH}$ AND $P_{i,n-1} > \tau_{CH}$

This evaluation can be done in a distributed fashion, by exchanging local messages. (For our simulations, if multiple nodes meet the above criteria, a node is randomly selected from the list). After the C-ACK transmission, the DATA transmission is triggered. Details on how the CH-based MAC scheme operates are shown in the Timing Diagram below.

8.2.2 OLA Size Adaptation Mechanism

OLA Size Adaptation is a link repair protocol defined to create a new link in a OLA unicast flow when the existing link is no longer available due to a *permanent* or *transient* change. A transient change could be when a portion of the OLA is being suppressed by another flow, this is a transient change because the nodes become available after the end of the other transmission. A permanent change is when a portion of nodes become permanently unavailable. This is generally called a network partition. Ad hoc networking applications such as battlefield and disaster recovery communications, environmental monitoring, and wide area surveillance are prone to partitions. Partitions can develop because of node mobility, limited radio power, node failure, uneven deployment, and obstacles like hills or walls. For both transient and permanent failures, an OLA Size Adaptation Mechanism is triggered after 3 retries. OLA size-adaptation is a link layer mechanism that grows a large enough OLA to go over the partition based on triggers/ cues received from the CH-based MAC scheme. These schemes require no centralized control.

Most of the existing multi-hop ad hoc routing protocols will work only for transient changes, and will fail to deliver messages when a partition occurs, when the width of the partition is greater than the transmission range of a node. Most of the works hence has been in designing proactive schemes [36] that prevent node partitioning by efficient routing

schemes. The only reactive partition recovery mechanism proposed is a ferrying scheme proposed in [37]. However ferrying schemes are not feasible in static WSNs. To the best knowledge of the authors, this is the only distributed network partition recovery scheme proposed for static wireless networks.

8.2.3 Data Link Layer Design: Timing Diagrams

The first part of this section lists the control messages used in the CH-based ACK scheme, and the OLA Survivability Scheme. The second section explains the timing diagrams for both the protocols.

8.2.3.1 Control Messages for Data Link Layer Design

The MAC Design and Survivability Scheme are achieved using the following control messages:

- RTS (Request to Send Frame) is simply the control message sent by nodes in the transmitting OLA wishing to send a DATA packet. OLA transmission that is decoded by nodes in the downstream direction because of omni-directional antennas, even though the signal is intended to travel upstream. The RTS specifies the address of the Destination OLA and the time for packet transmission.
- CTS (Clear to Send Frame) is a control message sent by the nodes in the receiving OLA, that received the RTS message, and were able to correctly decode it. The CTS specifies the time of DATA transmission. Any other node receiving the RTS or CTS frame should refrain from sending data for the time specified in the RTS/ CTS frame.
- CTS-RPT is a short control message sent by the CH to notify nodes in its OLA that the

CTS has been received for the RTS message that was sent.

- ACK-RPT is a short control message sent by the CH to notify nodes in its OLA that an ACK message has been received for the DATA packet that was sent.
- ReTx-RQT is a short control message that the CH sents out to nodes in its OLA to notify them that (a) the ACK hasn't been received even after the retries, and (b) the OLA Size Adaptation mechanism needs to be triggered.
- ReTx: DL^{n-1} nodes that decoded the original message and ReTx-RPT transmit ReTx to recruit more nodes from the same level. ReTx includes the original data payload.

8.2.3.2 Timing Diagrams

Figures 25 and 26 show the timing diagrams for the Custer Head-based ACK scheme, and Figure 27 illustrates the OLA Size Adaptation Mechanism for OLA flows. (The Timing Diagram is explained for OLAROAD, but could be extended to OLACRA as well). The vertical axis indicates time slots and the horizontal axis shows the upstream levels (Timing Diagrams are explained in the context of OLAROAD). For example T4 at UL^n in Figure 25 shows the activities of UL^n nodes in the fourth time interval. The different messages are color- and line-coded as shown in the legend. Figure 25 shows the operation when CTS/ACK is successfully received by the Cluster Head after sending an RTS/ DATA packet. The color coding used for all the timing diagrams is shown on the left. Figure 26 shows the case when a CTS/ACK is not received by the Cluster Head. Figure 27 illustrates the OLA Size Adaptation Mechanism.

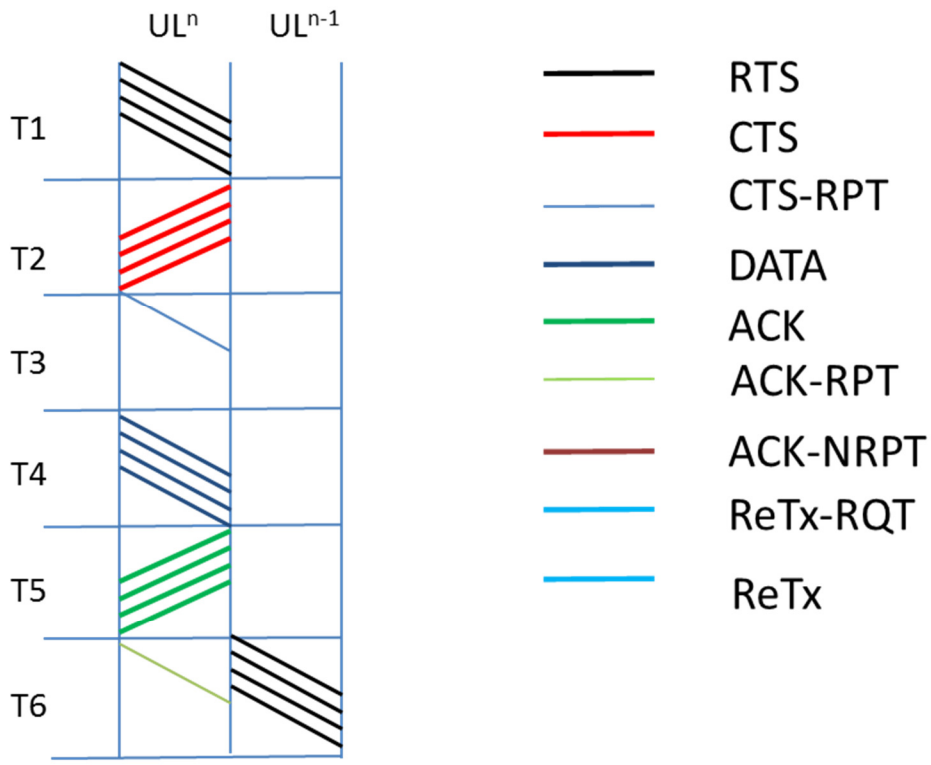

Figure 25: Timing Diagram (CTS and ACK successfully received by CH)

In Figure 25 at T1, nodes in UL^n (that have a DATA packet to transmit) transmit the CTS message. Nodes in UL^{n-1} that can decode the RTS will send CTS back at T2. The Cluster Head in UL^n is responsible for ensuring the CTS is received successfully. At T3, If the CH has received successfully it sends a CTS-RPT to nodes in UL^n. Nodes in UL^n, which didn't receive the CTS will make a note of this. At T4, all nodes in UL^n that transmitted the RTS and heard the CTS-RPT from CH will concurrently transmit the DATA message. At T5, the nodes in UL^{n-1} that receive the DATA, will transmit the ACK message. Similar to the CTS, the Cluster Head in UL^n is responsible for ensuring the ACK is received successfully. At T6, if the CH has received successfully it sends a ACK-RPT to nodes in UL^n. Nodes in UL^n, which didn't receive the ACK will make a note of this. It

should be noted that CTS-RPT and ACK-RPT are transmissions from a single node (CH) and intended to be received only within the hop. So at T6, while the CH in UL^n transmits the ACK-RPT, nodes in UL^{n+1} can transmit the CTS for forwarding the data packet.

Figure 26 shows the retry mechanism in OLA, when the CH doesn't receive an ACK/ CTS after transmitting the DATA/ RTS. . We don't consider failure modes cause due to node mobility, or incorrect Cluster Head selection. These would require a Cluster Head Re-selection; this is outside the scope of this study.

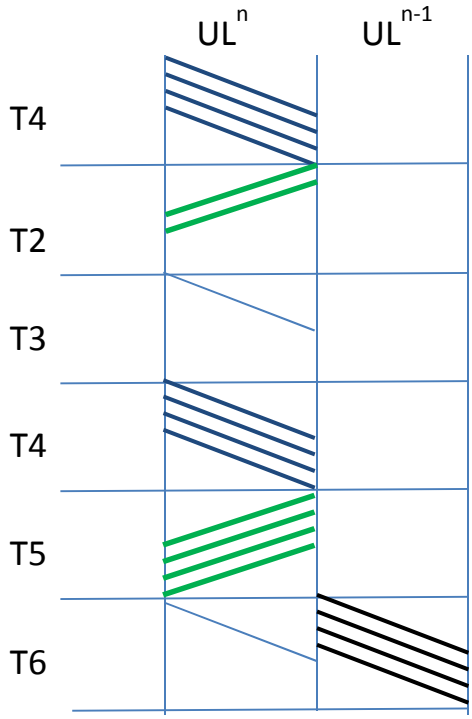

Figure 26: Timing Diagram (ACK not successfully received at Cluster Head).

Transmissions proceed normally till T4. At T5, only a few nodes in UL^{n-1} transmit the ACK. This could be because only a few nodes receive the DATA from UL^n, or because they are being suppressed by another flow/ hop. The CH does not receive the ACK,and hence initiates a ACK-NRPT. The purpose of the ACK-NRPT is to inform nodes in UL^n

that the ACK has not been received, and the DATA has to be retransmitted. All nodes that hear the ACK-NRPT, and transmitted the DATA at T4, retransmit the DATA at T7. At T8, nodes in UL^{n-1} that receive the DATA transmit the ACK. The ACK transmission is stronger this time, and the CH can decode it. The CH sends a ACK-RPT to nodes in its level to inform them that the ACK has been received. Transmissions progress as normal after this. Upon not receiving the ACK (or CTS), the CH tries for 3 times by resending the DATA (or RTS) in the current design. If it doesn't hear the ACK back after 3 retries, it initiates the OLA Size Adaptation Mechanism, which is explained next.

Figure 27 illustrates the OLA Size Adaptation Mechanism. We show the case when the CH doesn't receive an ACK even after 3 retries. In this situation, the CH realizes that the existing link is not reliable, and triggers the OLA Size Adaptation Mechanism. OLA Adaptation mechanism regrows the current link until it becomes reliable again. Like Figure 26, the CH repeats the DATA when it does not receive an ACK (this is shown in Figure 27 till T11). If it doesn't receive an ACK consecutively for 3 retries, the CH in UL^n transmits a ReTx-RQT at T12. Upon receipt of ReTx-RQT, the nodes in UL^n transmit ReTx. ReTx transmission at T13 is intended to recruit more nodes from the same level to relay the message so that their combined transmission can go around the hole in UL^{n-1} (or recruit more nodes in UL^{n-1} as the case maybe), thereby maintaining connectivity. Then in T14, all nodes in DL^{n-2} that ever decoded the original message (at T2 or T7) transmit together as an enlarged OLA. Finally, in T15, additional nodes in UL^{n+1} are able to decode the message, and they transmit an ACK. At T16, the CH notifies the nodes in UL^n of the receipt of ACK. If the CH still doesn't receive the ACK, it the Size Adaptation will recruit more nodes from UL^n till the link is reliable.

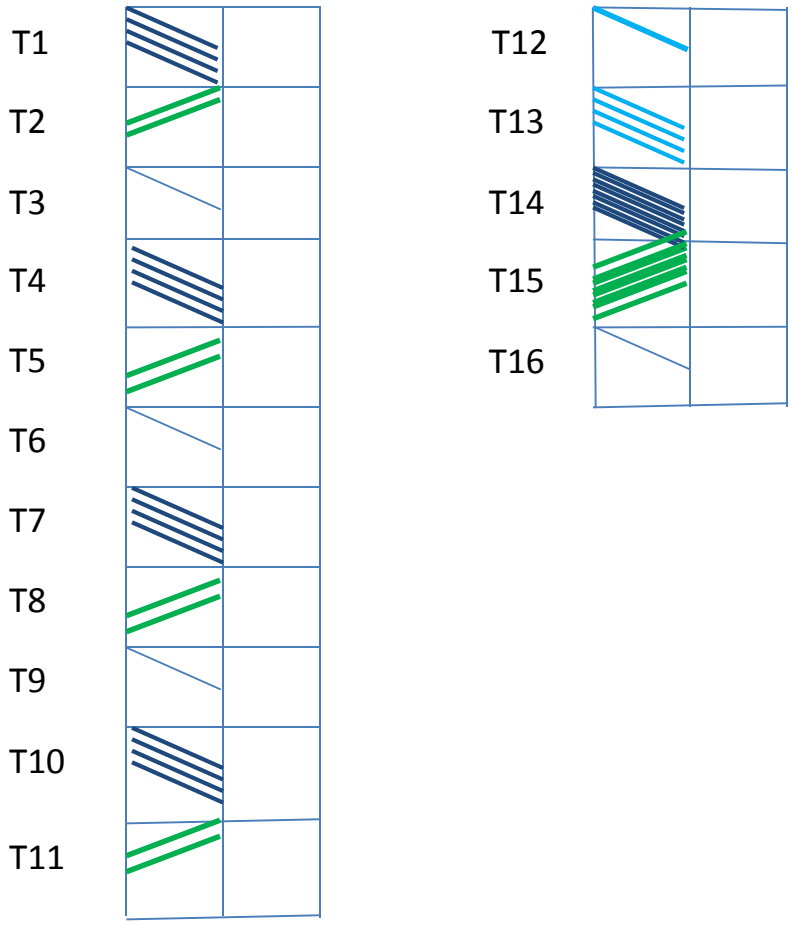

Figure 27: Timing Diagram (OLA Size Adaptation Mechanism)

It should be noted the OLA Size Adaptation mechanism increases node participation, and results in asymmetric contention regions across hops. If the original nodes that were suppressed start transmitting again (in case of a transient failure), the CH can detect it as it will see an increase in its received power of ACK (and CTS). At that point, the CH can limit the node participation in its level, scale back to its original size, thereby limiting node participation and associated contention region.

8.2.4 Transport Layer Access Scheme for OLA-based Networks

Even though the CH-based CSMA scheme enhances reliability for OLA flows, it

incurs a lot of overhead. In general, CSMA-based channel reservations might not be suitable for extremely energy constrained networks with very few packet transmissions. For such networks, a simple Transport Layer-based contention avoidance scheme where flows are scheduled sequentially, so that there is only a single flow within the network at any one time is proposed. The scheme basically treats the entire network as one big 802.11 (one hop basic service set). Since OLA flows are faster (i.e., they have lesser delay than a conventional multi-hop route) [4], treating one flow like one big hop is not so inefficient. When a node has a message to transmit and the medium is free it sends a request to send (RTS) to the sink using OLACRA. The RTS is a small message that contains information about the type of data being reported and also the duration of the transmission. The sink broadcasts a clear to send (CTS) on receipt of the RTS using OLA-T with the identity of the upstream source node and also the duration of the transmission. All the nodes in the network delay their transmissions by that time period. Even though the proposed scheme is very simple, it is of practical significance since most of the data transmitted in WSNs is not time-sensitive and hence the additional delay does not degrade the network performance significantly. Additionally, it consumes very less power and hence is suitable for energy constrained networks like tactical MANETs, intra-vehicular networks etc.

8.3 PERFORMANCE RESULTS

Each Monte Carlo trial has 5000 static nodes randomly distributed in an area of dimension 100 m X 100 m. For the first flow, the Sink is located at (20 m, 20m) and the upstream source node is located at (80 m, 20m). For experiemnts with two flows, the second flow is located at (20+x m, 20 m) and (80+x m, 20m), where x is a random number

varied in the simulation. Receiver Sensitivity of -90 dBm and a carrier sensing threshold of -100 dBm are assumed. Data rate of 250 kbps, and packet size of 128 bytes is used for the simulation (based on the IEEE 802.15.4 standard). An inter-packet spacing of 13 ms is used (which is approximately 3 times the packet duration, and is a common assumption in ad hoc networks). Downstream levels are established using OLA-T with source power P_s = -57 dBm. Step-size optimization is done in the downlink to obtain downlink levels with fixed step-sizes. For the uplink, the transmission powers are chosen such that the total number of hops from the Source to the Destination is the same for OLACRA and the non-CT scheme. The source and relays transmit at -40 dBm in the non-CT scheme. The source power is -47 dBm and the relay transmit power is -50 dBm for the OLA schemes.

For the Data Link Layer, channel reservation using CH-based MAC layer is implemented for OLA flows. For the multihop non-CT scheme, IEEE 802.11-based MAC is implemented. For link repair, OLA Size Adaptation is implemented in OLA, and AODV-based link repair is implemented for the non-CT flow.

To understand the operation of the CH-based MAC mechanism, and how OLA operates with multiple flows, Figure 28 considers two flows in the network. The distance between the flows, 'x' is varied as part of the simulation. We consider 4 cases of separation between the two flows: (1) *No overlap:* Here the two flows don't fall in to each other's suppression region for both OLA and non-CT. This gives us an idea of how the end to end delay of the CH-based MAC scheme compares with a non-CT multihop scheme when there is no inter-flow interference, (2) *PartialOverlapI:* Here a small portion (10 %) of the nodes in Flow 1 are under the suppression region of Flow 2 in OLA, (3) *PartialOverlapII:* Here a larger portion (39 %) of nodes in Flow 1 are under the suppression of Flow 2 in OLA, (4) *Full*

Overlap: Here Flows 1 and 2 are fully under the suppression of each other in both OLA and non-CT.

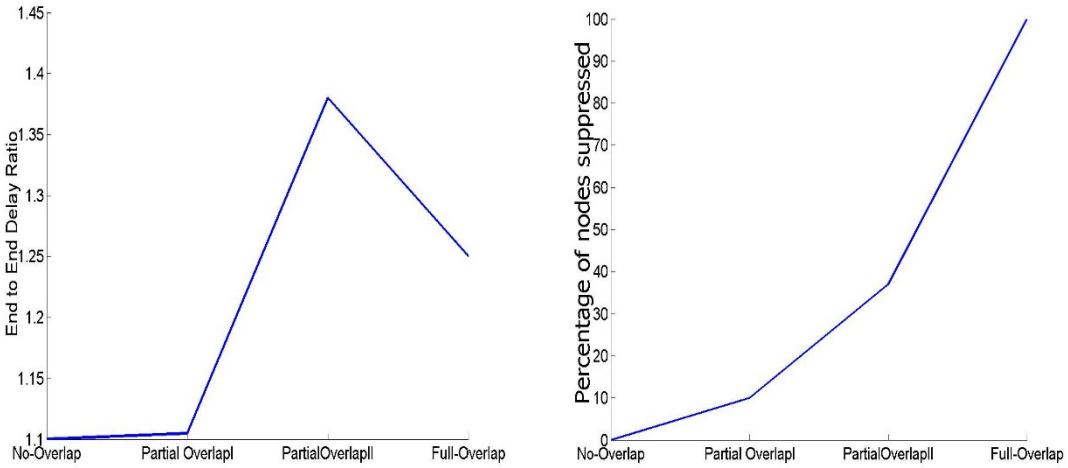

(a) (b)

Figure 28: (a) End to End Ratio, and (b) Percentage of Nodes Suppressed in HOLA versus non-CT

It can be seen that the end-to-end delay for OLA is higher than non-CT in all the cases. This is because of the additional control message exchanges by the Cluster Head in OLA (It should be noted that the OLA flows and non-CT flows have been designed to have the same number of hops, and OLA nodes transmit at a much lower power). The No-overlap case and Full Overlap case have similar (and slightly higher than non-CT) end-to-end delays. For the PartialOverlapI case, the increase in end-to-end delay compared to the Non-Overlap case is trivial, whereas its significant for the PartialOverlapII case. This is happening because of the following reasons. For the PartialOverlapI case, ther nodes that are suppressed are the side nodes. As seen earlier, the side nodes don't have a significant impact on the reliability, and hence doesn't affect the end-to-end delay. However, for

PartialOverlapII case, more nodes are suppressed, and hence this affects the Link Reliability.

8.3.1 OLA Size Adaptation Mechanism

In this section, we demonstrate the benefits of our proposed "Network Survivability Protocol" in disconnected networks where partitions have occurred either due to nodes depleting their energy or natural obstacles in the network. We assume the deterministic channel. Each Monte Carlo trial has nodes randomly distributed in a square field of dimensions 34 × 34 units with the Sink located at the center. The nodes are assumed to be static. For all results in this section, $\tau d = 1$ and 400 Monte Carlo trials are performed. The downstream levels are established using OLA-T with source power $Ps = 2$ and relay power $Pr = 0.5$. The upstream source node is located at a radius of 19 and a relay power of 1 is used for the upstream transmission. The multi-hop transmission is however assumed to be at a higher power of 2. The multi-hop route is chosen to be the route having the minimum number of hops between the Source and Destination, which is the case in popular multi-hop routing schemes like DSR [30].

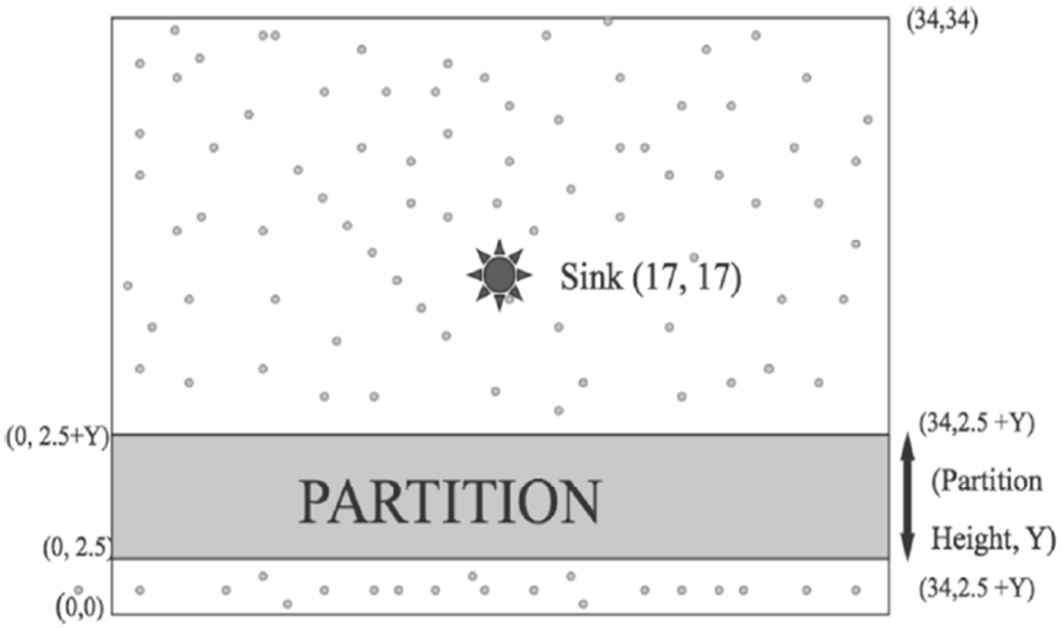

Figure 29: Illustration of Network Partition

We consider a Complete Partition as shown in Figure 29 that cuts through the network and divides it in two. As a part of our simulation we let the partition height, *Y* (as shown in Figure 29) be 0, 5, 10 or 15 units. Figure 30, shows the variation of the Packet Delivery Ratio (PDR) with the partition height for 3 cases. The first case that we consider is the multi-hop routing scheme. The other two cases, "early partition" and "late partition," have been considered to show two different kinds of partitions. In early partition we assume that the partition already existed in the network before the nodes were deployed, which will be the case if the partition is due to a natural obstacle like a wall. In the other case, late partition, the assumption is that the partition is created sometime after the nodes are deployed and initialization of OLACRA has been carried out. This will be the case if the partition is caused due to nodes depleting their energy. We can see that the scheme fails to maintain connectivity even at partition heights of around 3 units. For the late partition case,

we get a high PDR of close to 1 even at a height of 15 units. However for the late partition case the PDR begins to fail around 10 units. This is because the partition is so big that downlink levels fail to form in OLA-partition case. It also means that if the downlink levels have been created by the initialization phase, our size-adaptation mechanism is intelligent enough to overcome partitions of very large dimensions.

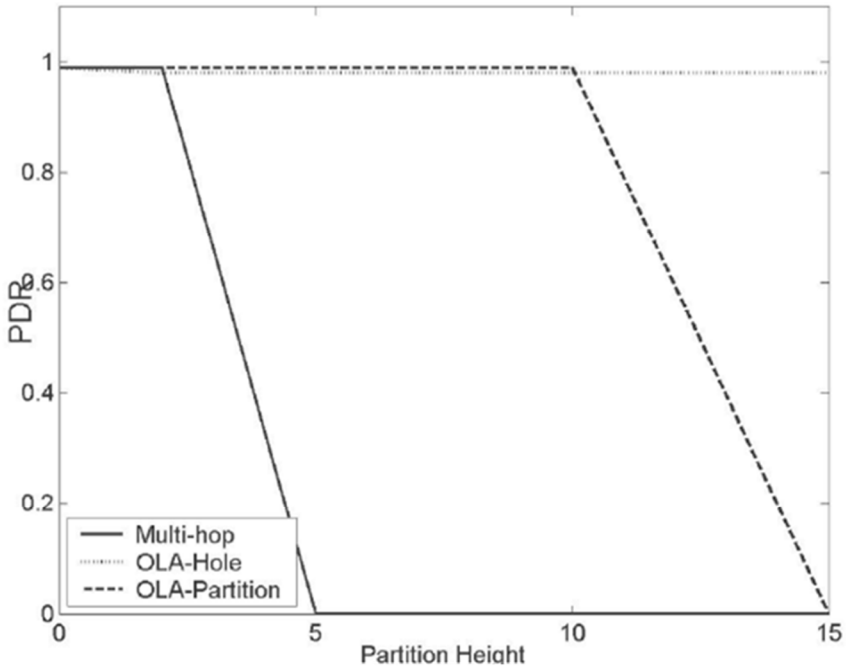

Figure 30: PDR versus partition height for OLA and multihop unicast schemes

CHAPTER 9

CONCLUSIONS

The focus of this dissertation has been to investigate a simple, distributed form of cooperative transmission called Opportunistic Large Array (OLA) as a means to address some of the challenges of distributed unicast routing in multi-hop wireless networks. The OLA derives a signal-to-noise ratio (SNR) advantage from the spatial diversity of distributed single-antenna radios. The unique capabilities that OLAs provide for improving link quality, energy efficiency, and resistance to mobility were analyzed as part of the dissertation. In this context, the dissertation makes four main contributions each of which are further discussed below:

(1) A distributed routing scheme, OLACRA, for static wireless sensor networks,

(2) A scalable and reactive routing protocol, OLAROAD, for mobile ad hoc networks,

(3) A distributed Data Link Layer design suitable for OLA unicast networks, and

(4) An adaptive and distributed route recovery scheme, OLA Size Adaptation, suitable for OLA networks.

In the context of static WSNs, we first explain the need for a distributed, low overhead and energy efficient routing scheme in wireless sensor networks by highlighting the use cases and unique requirements for certain wireless sensor network applications. Based on this, we present an algorithm called OLACRA, which is the first OLA-based unicast routing scheme that has been proposed for wireless sensor networks. OLACRA

requires no centralized control for route setup and relay coordination, and involves no individual addressing of relays. Our results show that as network node degree increases, the network overhead and route performance remain constant for high-density networks in OLACRA, while the network overhead increases and performance degrades with node degree in non-OLA CT schemes. Because OLA-based protocols limit node participation significantly compared to the OLA-broadcast schemes, our simulation results indicate that network energy savings of approximately 80 percent is observed relative to broadcast-based OLA schemes. This results in a longer sensor lifetime, which is an important performance metric in certain WSN applications.

In the context of multi-hop mobile ad hoc networks, we considered the problem of achieving route reliability with increasing density and mobility. We considered the use of OLA-based physical layer to achieve virtual MIMO links in a reactive route. Based on this premise, we present OLAROAD, which is a reactive routing protocol that achieves route reliability in mobile networks. OLAROAD routes comprise a series of clusters that cover a significant area. Node density variations (as long as the node density is above a specified minimum), and low node mobility's have little effect on the cluster areas; hence the need for rerouting and corresponding overhead is not present in OLAROAD for a single flow network. The performance of OLAROAD was evaluated using an enhanced Physical layer simulator that captured the effects of concurrent cooperative transmissions. Specifically, we investigated how the physical layer benefits of OLA would translate to network layer performance improvements. We demonstrated that the improvements achieved with this strategy are non-trivial: OLA routes have a lower end-to-end delay, lower route formation time, and are independent of density variations, in comparison with the state-of-art multi-

hop strategies. These features make OLA routing suitable for networks that have random topological changes like intra-vehicular networks.

The third contribution of the dissertation is a Cluster Head-based MAC scheme for OLA networks. We analyzed the suppression regions and suppression times of OLA hops, and demonstrated that unlike non-CT networks, the suppression regions of OLA hops were asymmetric and depend on the hop and level index. Based on this, we identified the challenges in designing the Data Link Layer for OLA physical layer. The performances of standard 802.11 MAC schemes based on CSMA were analyzed for OLA; our results indicated that they are not feasible for OLA routing. We presented a Cluster-Head-based solution that with intelligent scheduling algorithms achieves a fine balance between scalability/ overhead and reliability in WSNs. Through multiple iterations of the simulations, the gains of the proposed solution under different network conditions were illustrated. We compare the reliability of the proposed scheme and AODV. We show that comparable reliabilities can be achieved in OLOROAD at the expense of a higher overhead. Even though CH-based handshake scheme has the additional overhead of selecting the cluster head, it avoids the additional delay and overhead that would occur when trying to achieve consensus among the nodes in the OLA.

Lastly, this dissertation presents the OLA Size Adaptation Mechanism, an adaptive route recovery scheme, which generates large enough cooperating transmitter sets that can circumvent network holes (partitions in the network caused by, e.g., nodes dying, which pose a significant threat to WSN deployments, without requiring any centralized control. While majority of the previous works in this area try to prevent the formation of network holes, this work is the first, to our knowledge, that uses cooperative transmission to create

reliable transmission paths on networks that have been made dysfunctional by network holes. We show that the reliability of route recovery in for the proposed scheme depends on the power density product of an area, as opposed to the individual transmit powers of nodes. We demonstrate that this feature allows the network to remain operational over lower transmit powers relative to Non-CT multihop networks. Even though, OLA Size Adaptation mechanism can overcome network holes, it would create large and asymmetric OLAs. The CH-based handshake schemes proposed in this dissertation would need to be extended to address the asymmetry in these routes.

There are many directions for future research. In this dissertation, we provided several novel approaches that were each optimized under a different set of assumptions, for example the objective of routing protocol design in OLACRA was to ensure no nodes had to be addressed individually, however the objective in CH-based handshaking was to ensure link reliability and this required the cluster head nodes to be addressed. Before these approaches can be used a practical protocol, they should be integrated together and jointly optimized.

CHAPTER 10

FUTURE WORK

While the dissertation illustrates how distributed OLA schemes could be used to improve energy efficiency and reliability in distributed wireless networks, there exist several interesting open problems that are topics for future research.

1. The OLA-based protocols that have resulted from this Ph.D. work, namely OLACRA-SC, OLAROAD for upstream communication, and their variants have been analyzed using detailed simulation models mainly for deterministic path loss models. Subsequent research directions include a detailed theoretical analysis of the protocol for random node deployments, under fading and shadowing wireless environments. In addition to this activity, channel modeling needs to be done for some of the applications that OLA routing is applicable for, and OLA protocols need to be analyzed for those channel models as well.

2. The current work addresses the challenges in MAC layer design and handshaking when there are multiple hops per flow, and proposes a simple MAC scheme that operates in these networks. However, consideration of issues such as collisions and multiple intersecting flows needs to be considered and the Data Link Layer design needs to be adapted for this.

3. Heterogeneous networks: While the dissertation focuses on homogeneous networks where all the sensor nodes and access points are equipped with similar antenna and computing capabilities, actual deployments in many applications are likely to be heterogeneous in the capabilities of nodes in the network. This heterogeneity makes

distributed algorithms more challenging since resource capabilities are varied across the network. In practice, this would increase the asymmetry induced problems identified in this dissertation. This is especially relevant in the design of medium access control solutions for wireless networks with node cooperation. Distributed carrier sensing, accounting for asymmetric link interference and appropriate link reliability mechanisms are important and more challenging in such contexts. The OLA-based protocols and Data Link Layer proposed in this dissertation needs to be extended to heterogeneous networks.

4. Handling mobility: The solutions developed in this dissertation have mainly focused on static and low mobility users for a single packet transmission. For such case, the effect of mobility on intra and inter hop interferences is relatively low. However for highly mobile users, the contention regions and hence network throughput varies fast and hence the stability of OLA routing would degrade with mobility. Investigating this line of research and developing solutions that explicitly handle user mobility is an interesting avenue for future research.

CHAPTER 11

PUBLICATIONS

JOURNAL PAPERS

1. L. Thanayankizil, A. Kailas, and M. A. Ingram, "Routing Protocols for Wireless Sensor Networks that have an Opportunistic Large Array (OLA) Physical Layer," in *Ad-Hoc & Sensor Wireless Networks: An International Journal (Special Issue on 1st International Conference on Sensor Technologies and Applications)*, Dec. 2008.

2. L. V. Thanayankizil, A. Kailas, and M. A. Ingram, "Opportunistic large Array Concentric Routing Algorithm (OLACRA) for Upstream Routing in Wireless Sensor Networks," *submitted* to *IEEE JSAC(Special Issue on Wireless Sensor Networks and Applications)*, April 2009.

3. A. Kailas, L. Thanayankizil, and M.A. Ingram, "A simple cooperative transmission protocol for energy-efficient broadcasting over multi-hop wireless networks," in *KICS/IEEE Journal of Communication and Networks* (Special Issue on Wireless Cooperative Transmission and Its Applications), vol.10, no. 10, pp 213-20, June 2008.

BOOK CHAPTERS

1. M. A. Ingram, L. Thanayankizil, J. W. Jung, and A. Kailas, " Energy-Harvesting Wireless Sensor Networks," in *Globalization of Mobile and Wireless Communications: Today and in 2020*, Springer-Verlag, 2009.

CONFERENCE PAPERS

1. L. Thanayankizil and M. A. Ingram, "Reactive Robust Routing with Opportunistic Large Arrays," in *Proc. of IEEE International Conference on Communications (ICC)*, Dresden, Germany, June 14-18, 2009.

2. L. Thanayankizil, and M. A. Ingram, "Reactive routing for multi-hop dynamic ad hoc networks based on opportunistic large arrays," in *Proc. 51st Annual IEEE GLOBECOM*, New Orleans, Nov. 24-30, 2008.

3. L.Thanayankizil and M. A. Ingram, "A Two-hop ACK Scheme for ensuring survivability in a cooperative transmission network," in *Proc. of WPMC* , Jaipur, Dec 2007.

4. L. Thanayankizil, and M. A. Ingram, "Opportunistic Large Array Concentric Routing Algorithm (OLACRA) over Wireless Fading Channels," in *Proc. of 50th Annual IEEE GLOBECOM*, Washington, DC, Nov. 26-30, 2007.

5. A. Kailas, L. Thanayankizil, and M. A. Ingram, "Power Allocation and Self-Scheduling for Cooperative Transmission Using Opportunistic Large Arrays," in *Proc. 26th Annual IEEE MILCOM*, Orlando, FL, Oct. 29-31, 2007.

6. L. Thanayankizil, and M. A. Ingram, "Energy-Efficient Strategies for Cooperative Communications in Wireless Sensor Networks," in *Proc. IEEE SENSORCOMM*, Valencia, Spain, Oct. 14-20, 2007 [IEEE Best Paper]

7. L. Thanayankizil, and M. A. Ingram, "Two Energy-Saving Schemes for Cooperative Transmission with Opportunistic Large Arrays," in *Proc. 50th Annual IEEE GLOBECOM*, Washington-DC, Nov. 26-30, 2007.

REFERENCES

[1] A. Sendonaris, E. Erkip, and B. Aazhang, "User Cooperation – part 1: System Description, part ii: Implementation Aspects and Performance Analysis," in *IEEE Trans. On Communication*, vol. 51, no. 11, pp. 1927–1948, Nov. 2003.

[2] J. N. Laneman, D. Tse, and G. W. Wornell, "Cooperative Diversitry in Wireless Networks: Efficient Protocols and Outage Behaviour," in *IEEE Trans. On Information theory Theory*, vol. 50, no. 12, pp. 3063–3080, Dec. 2004.

[3] J. N. Laneman and G. W. Wornell, "Distributed Space-Time Coded Protocols for Exploiting Cooperative Diversity in Wireless Networks," in *Proc. IEEE Global Comm. Conf. (GLOBECOM)*, Taipei, Taiwan, Nov. 2002, pp. 77-81.

[4] A. Scaglione, and Y. W. Hong, "Opportunistic large arrays: Cooperative Transmission in Wireless Multi-hop Ad hoc Networks to Reach Far Distances," in *IEEE Trans. On Signal Processing*, vol. 51, no. 8, pp. 2082–92, Aug. 2003.

[5] B. Sirkeci Mergen and A. Scaglione, "Asymptotic Analysis of Multi-Stage Cooperative Broadcast in Wireless Networks," in *Proc. INFOCOM*, Mar. 2005, pp. 2755-2763.

[6] Hong Y.W.; Scaglione A. "Energy-Efficient Broadcasting with Cooperative Transmission in Wireless Sensory Ad Hoc Networks", in *Proc. of the Allerton Conference*, Monticello IL, Oct 2003.

[7] R. Mudumbai, G. Barriac, and U. Madhow, "Spread-spectrum techniques for distributed space-time communication in sensor networks," in *Proc. of the 38th Asilomar Conference on Signals, Systems and Computers (invited paper),* Pacific Grove, CA, Nov. 7--10, 2004, pp. 908-912 vol. 1.

[8] A. Khisti, U. Erez, and G.W. Wornell, "A Capacity Theorem for Cooperative Multicasting in Large Wireless Networks," in *Proc. Allerton Conf. Commun., Contr., and Computing*, (Illinois), Oct. 2004.

[9] J. Wieselthier, G. Nguyen, and A. Ephremides, "On the Construction of Energy-Efficient Broadcast and Multicast Trees in Wireless Networks," in *Proc. INFOCOM*, Mar. 2000, pp. 585-594.

[10] L. V. Thanayankizil, A. Kailas, and M. A. Ingram, " Energy-Efficient Strategies for Cooperative Communication in Wireless Sensor Networks," in *Proceedings of IEEE SENSORCOMM*, Valencia, Spain, Oct. 14-20, 2007.

[11] L. V. Thanayankizil, and M. A. Ingram, "Opportunistic Large Array Concentric Routing Algorithm (OLACRA) over Wireless fading Channels ," in *Proceedings of 50th Annual IEEE GLOBECOM*, Washington, DC, Nov. 26-30, 2007.

[12] A. Kailas, L. Thanayankizil and M. A. Ingram, "A Simple Cooperative Transmission Protocol for Energy-Efficient Broadcasting Over Multi-Hop Wireless Networks," in *Journal of Communications and Networks (Special Issue on Wireless Cooperative Transmission and Its Applications)*, vol. 10, no. 2, pp. 1-8, Jun 2008.

[13] A. Kailas, L. Thanayankizil, and M. A. Ingram, "Power Allocation and Self-Scheduling for Cooperative Transmission Using Opportunistic large Arrays," in *Proceedings of 26th Annual IEEE MILCOM*, Orlando, FL, Oct. 29-31, 2007.

[14] L. V. Thanayankizil, and M. A. Ingram, "Opportunistic Large Array Concentric Routing Algorithm (OLACRA) over Wireless fading Channels ," in *Proceedings of 50th Annual IEEE GLOBECOM*, Washington, DC, Nov. 26-30, 2007.

[15] S. Singh, M. Woo and C. S. Raghavendra, "Power-Aware Routing in Mobile Ad Hoc Networks", in Proceedings of *ACM/IEEE MOBICOM,* Orlando, FL, Oct. 29-31, 1998.

[16] S. Banerjee, A. Misra , "Minimum Energy Paths for Reliable Communication in Multi-hop Wireless Networks", in *Proc. of MobiHoc 2002*, Lausanne, Switzerland, June 2002.

[17] V. Rodoplu and T.H.Meng, "Minimum energy mobile wireless networks," in *IEEE J. Selected Areas in Communications*, 17(8): 1333-1344, August 1999.

[18] J. H. Chang and L. Tassiulas, "Maximum lifetime routing in wireless sensor networks," in *Proc. of ATIRP Conference*, College Park, MD, Mar. 2000.

[19] J. H. Chang and L. Tassiulas, “Energy conserving routing in wireless ad-hoc networks,” in *Proc. IEEE INFOCOM*, pp. 22–31, March 2000.

[20] A. Misra, S. Banerjee, “ MRPC: Maximizing Network Lifetime for Reliable Routing in Wireless Environments,” in IEEE *Wireless Communications and Networking Conference (WCNC)*, Orlando, Florida, March 2002.

[21] J. Park, S. Sahni, “Maximum Lifetime Broadcasting in Wireless Networks,” in *IEEE Trans. Computers* 54(9): 1081-1090 (2005).

[22] S. Savazzi and U. Spagnolini, “Energy aware power allocation strategies for multi-hop cooperative transmission schemes,” in *IEEE Journal on Selected Areas in Communications*, pp. 318-327, February 2007.

[23] X. Fang, T. Hui, Z. Ping and Y. Ning, “Cooperative routing strategies in ad hoc networks” in *IEEE Vehicular Technology Conference*, 2005. VTC 2005-Spring. 2005.

[24] B. Gui, L. Dai, and L.J. Cimini Jr., “Routing Strategies in Multihop Cooperative Networks,” in *IEEE Wireless Communications and Networking Conference (WCNC)*, Las Vegas, March 2007.

[25] G. Jakllari, S. V. Krishnamurthy, M. Faloutsos, and P. V. Krishnamurthy, “On Broadcasting with Cooperative Diversity in Multi-Hop Wireless Networks,” in *IEEE Journal On Selected Areas In Communications*, February 2007.

[26] B. Sirkeci Mergen, A. Scaglione, and G. Mergen, “A continuum approach to dense wireless networks with cooperation,” in *Joint special issue of the IEEE Transactions on Information Theory and IEEE/ACM Trans. On Networking*, Vol. 25, No. 2, June 2006.

[27] E. Biagioni, “Algorithms for Communication in Wireless Multi-Hop Ad Hoc Networks Using Broadcasts in Opportunistic Large Arrays (OLA),” in *Proc. ICCCN*, Aug. 07, pp. 1111–16.

[28] S. Wei, D.L. Goeckel, and M. Valenti, “Asynchronous cooperative diversity,” in *Proc. of CISS*, Mar. 2004.

[29] Zhang, Tsatsanis and Sidiropoulos, “Performance analysis of a random access packet radio system with joint network-spatial diversity,” in *Proceedings of ICASSP,* March 2000.

[30] C.E. Perkins, E.M. Belding-Royer, “Ad hoc On-Demand Distance Vector Routing,” In *Proc. of the 2nd IEEE Workshop on Mobile Computing Systems and Applications*, New Orleans, February 1999, pp. 90-100.

[31] J. Broch, D. A. Maltz, D. B. Johnson, Y.-C. Hu, and J. Jetcheva, “A performance comparison of multi-hop wireless ad hoc network routing protocols,” in *Proc. of Mobile Computing and Networking* , 1998, pp. 85–97.

[32] H. Kim and R. Buehrer, “A Technique to Exploit Cooperation for Packet Retransmission in Wireless Ad Hoc Networks,” in *Journal of Communications and Networks (Special Issue on Wireless Cooperative Transmission and Its Applications)*, vol. 10, no. 2, pp. 48-55, Jun 2008.

[33] S. Biswas , R. Morris, “Opportunistic routing in multi-hop wireless networks,” in *ACM SIGCOMM Computer Communication Review*, v.34 n.1, January 2004.

[34] M. Kurth, A. Zubow and J. Redlich, “Cooperative Opportunistic Routing using Transmit Diversity in Wireless Mesh Networks,” in *IEEE INFOCOM*, 2008.

[35] L. V. Thanayankizil, A. Kailas, and M. A. Ingram, “Opportunistic large Array Concentric Routing Algorithm (OLACRA) for Upstream Routing in Wireless Sensor Networks,” *submitted* to *IEEE JSAC*, April 2009.

[36] K. Sanzgiri, I. Chakeres and E. Belding-Royer, “ Pre-Reply Probe and Route Request Tail: Approaches for Calculation of Intra-Flow Contention in Multihop Wireless Networks" in *Mobile Networks and Applications (MONET) Journal*, 11(1), pp. 21-35, February 2006

[37] K. Sanzgiri, I. Chakeres and E. Belding-Royer, "Determining Intra-Flow Contention along Multihop Paths in Wireless Networks," in *Proceedings of Broadnets Wireless Networking Symposium*, San Jose, CA, October 2004.

[38] T. R. Halford and K. M. Chugg, "The stability of multihop transport with autonomous cooperation," in *MILCOM'11*, Baltimore, MD, November, 2011.

[39] T. R. Halford and K. M. Chugg, "The reliability of multihop routes with autonomous cooperation," UCSD Information Theory and Applications Workshop (invited), La Jolla, CA, February, 2011.

[40] H. Jung, M. Ingram, “Analysis of Spatial Pipelining in Opportunistic Large Array Broadcasts,” in *MILCOM 2011*, Baltimore, MD, November 2011.

[41] Y. Chang, H. Jung, and M. Ingram, “Demonstration of an OLA-based Cooperative Routing Protocol in an Indoor Environment,” in *European Wireless*, Vienna, Austria, April 2011.

[42] R. Hariharan, H. Hassanieh, and D. Katabi, "SourceSinc: A Distributed Wireless Architecture for Exploiting Sender Diversity," in *ACM SIGCOMM,* August 2010